



ALMA MATER STUDIORUM  
UNIVERSITÀ DI BOLOGNA

ARCHIVIO ISTITUZIONALE  
DELLA RICERCA

Alma Mater Studiorum Università di Bologna  
Archivio istituzionale della ricerca

3D geological modelling of the Bologna urban area (Italy)

This is the final peer-reviewed author's accepted manuscript (postprint) of the following publication:

*Published Version:*

Giacomelli S., Zuccarini A., Amorosi A., Bruno L., Di Paola G., Martini A., et al. (2023). 3D geological modelling of the Bologna urban area (Italy). *ENGINEERING GEOLOGY*, 324, 1-19 [10.1016/j.enggeo.2023.107242].

*Availability:*

This version is available at: <https://hdl.handle.net/11585/962973> since: 2024-03-11

*Published:*

DOI: <http://doi.org/10.1016/j.enggeo.2023.107242>

*Terms of use:*

Some rights reserved. The terms and conditions for the reuse of this version of the manuscript are specified in the publishing policy. For all terms of use and more information see the publisher's website.

This item was downloaded from IRIS Università di Bologna (<https://cris.unibo.it/>).  
When citing, please refer to the published version.

(Article begins on next page)

10 August 2024

This is the final peer-reviewed accepted manuscript of:

Giacomelli S.; Zuccarini A.; Amorosi A.; Bruno L.; Di Paola G.; Martini A.; Severi P.; Berti M.: *3D geological modelling of the Bologna urban area (Italy)*

ENGINEERING GEOLOGY

VOL. 324

ISSN 0013-7952

DOI: [10.1016/j.enggeo.2023.107242](https://doi.org/10.1016/j.enggeo.2023.107242)

The final published version is available online at:

<https://dx.doi.org/10.1016/j.enggeo.2023.107242>

Terms of use:

Some rights reserved. The terms and conditions for the reuse of this version of the manuscript are specified in the publishing policy. For all terms of use and more information see the publisher's website.

This item was downloaded from IRIS Università di Bologna (<https://cris.unibo.it/>)

**When citing, please refer to the published version.**

### **3D geological modelling of the Bologna urban area (Italy)**

*Giacomelli S.<sup>1,4\*</sup>, Zuccarini A.<sup>1</sup>, Amorosi A.<sup>1</sup>, Bruno L.<sup>2</sup>, Di Paola G.<sup>1</sup>, Martini A.<sup>3</sup>, Severi P.<sup>3</sup>, Berti M.<sup>1</sup>*

<sup>1</sup>Department of Biological, Geological, and Environmental Sciences (BiGeA), University of Bologna, Via Zamboni 67, Bologna, Italy

<sup>2</sup>Department of Chemical and Geological Sciences, University of Modena and Reggio Emilia, Via Giuseppe Campi 103, Modena, Italy

<sup>3</sup>Geologic, Soil, and Seismic Survey – Emilia-Romagna Region, Viale Aldo Moro 30, Bologna, Italy

<sup>4</sup>ISPRA, Institute for Environmental Protection and Research, Via Vitaliano Brancati 48, Rome, Italy

\*Corresponding author

email: giacserena@gmail.com

full postal address: Via Zamboni, 67 - 40126 Bologna

\*Corresponding author present address: ISPRA, Institute for Environmental Protection and Research, via Vitaliano Brancati 48, Rome, Italy

### **Abstract**

Urban geological modelling plays a crucial role in facilitating the sustainable utilization of the urban subsurface and the development of effective strategies for geohazard mitigation. Traditionally, geological models of urban areas rely on lithological correlations of boreholes and well data. However, in complex depositional settings such as alluvial environments, where the standard concepts of superposition and lateral continuity of strata are often violated, lithostratigraphic correlation can be challenging even over short distances, leading to considerable uncertainty in the final geological model. Therefore, in such cases, lithofacies analysis can provide a more robust categorisation of subsurface geological units as lithofacies mainly reflect the depositional process, while their associations provide a reliable picture of sedimentary bodies and their geometries. In this work, we used the lithofacies correlation approach to develop a 3D geological model of the urban area of Bologna (Italy) where a complex, thick alluvial succession makes lithological correlations very difficult. To minimize subjectivity, we re-interpreted 940 existing borehole logs in terms of depositional facies and combined stratigraphic data with geophysical HSVR (Horizontal to Vertical Spectral Ratio) measurements and surface analysis (morphology and river network) based on a DTM (Digital Terrain Model). This led to the detailed reconstruction of the subsurface depositional architecture, forming the basis for the 3D geological model. The model revealed the presence of three

distinct depositional domains with different stratigraphic architectures. From west to east: Domain A (Reno River) corresponds to the gravel-dominated fill of a river valley abruptly passing to Domain B (Bologna urban area) that represents a morphological and stratigraphical divide, topographically elevated with respect to the surrounding areas and characterized by fine-grained deposits with frequent paleosols. Lastly, Domain C (Savena River) exhibits the typical alluvial fan pattern, marked by a gentle convex-up surface morphology with gravelly-sandy deposits with a low degree of lateral amalgamation. The geological model effectively explains the distribution of ground subsidence in Bologna since the 1960s, which is attributable to significant groundwater pumping. This is evident from the comparison of the model with both the ground displacement contours resulting from the 1983-1987 topographic levelling campaign and the subsidence rate map derived from the 2006-2011 Radarsat interferometric survey. Subsidence shows strong variations at the domains' boundaries, especially at the limit between Domain A (Reno River) where high values prevail, and Domain B (Bologna city centre) characterised by the lowest values.

**Keywords:** urban geological modelling; Bologna 3D model; alluvial stratigraphy; lithofacies correlation

## **1. Introduction**

Underground space has become increasingly important for the sustainable development of urban areas (Hooimeijer & Maring, 2018; Von der Tann et al., 2019) since it provides new construction space, saves land resources, alleviates the pressure on the surface, preserves cultural heritage, and absorbs in part environmental pollution (He et al., 2020; Volchko et al., 2020). The subsurface is also rich in geothermal resources that offer great potential for decarbonisation and is a major source of drinking water (Huggenberger & Epting, 2011; Hemmerle et al., 2022). Moreover, subsurface areas are less susceptible to natural disasters and can increase the resilience of future cities (Price et al., 2016). For these reasons, underground development is nowadays seen as the main path toward modern sustainable cities.

The key requirement for subsurface planning is a superior understanding of local geological conditions. A well-developed geological model is a prerequisite for obtaining reliable geotechnical, geomechanical, and hydrogeological models, as well as for assessing and mitigating natural hazards (El May et al., 2010; Culshaw & Price, 2012; Lapenna et al., 2020). Typically, urban subsurface models are built by combining

different types of data (boreholes, wells, geological maps, stratigraphic cross-sections, geophysical surveys) in order to understand the 3D distribution of geological units. Modelling strategies depend on the specific aims of the study, and different approaches have been used to balance user requirements with geological complexity and data availability (e.g., Thierry et al., 2009; Stafleu et al., 2011; Mathers et al., 2014; Fordyce & Campbell, 2017; Kokkala & Marinos, 2022). Regardless of the modelling procedure, the first and most important step is the subdivision of sedimentary sequences into homogeneous geological units. Different criteria can be used for this purpose, such as lithostratigraphy, chronostratigraphy, or biostratigraphy (Miall, 2016). Urban geological models are primarily based on lithostratigraphy. Lithostratigraphic units are differentiated based on the type of rock or soil, namely its composition and texture. Lithology is an objective parameter that can be easily derived from borehole descriptions and that is closely related to the mechanical, physical and hydrological properties of the material. For this reason, most published models employ this criterion to represent the urban subsurface.

However, in complex depositional environments, lithology-based stratigraphic correlation can be challenging. Alluvial deposits, in particular, consist of stacked sequences of coarse-grained sediments that commonly violate the standard concepts of superposition and lateral continuity of strata (Miall, 1985). In such cases, the sequence stratigraphic approach has the potential to overcome the limitations of lithostratigraphy. Sequence stratigraphy combines lithofacies analysis, biostratigraphy, and chronostratigraphy to subdivide sedimentary deposits into time-coherent packages (Van Wagoner et al., 1990; Posamentier & Allen, 1999; Catuneanu, 2006; Miall, 2016). The fundamental point of this approach is the recognition of stratigraphic surfaces that bound sedimentary facies (i.e., lithostratigraphic bodies) formed in specific depositional environments (e.g., floodplain, active channel, crevasse splay, etc.). Since depositional systems include facies tracts where the spatial distribution of lithostratigraphic units can be predicted, lithofacies provide a powerful framework for stratigraphic correlation beyond the simple lithologic approach and are widely employed in oil and gas exploration (Vail et al., 1977; Wornardt, 1993; Miall, 1996). Despite its potential, sequence stratigraphy received little attention in urban geology. This is probably attributed to the challenges in reconstructing lithofacies associations from borehole logs, which requires specific sedimentological expertise. Only a few studies used such a multidisciplinary approach to reconstruct urban subsurface (Velasco et al., 2012; Salvany & Aguirre, 2020).

In this work, we combine morphological, geophysical, and stratigraphic analyses to develop a 3D geological model of the city of Bologna, in northern Italy. Bologna is settled upon a hundred-metres thick alluvial succession with a complex internal architecture that makes traditional lithological correlation very difficult. A Digital Terrain Model (DTM) based analysis, combined with a detailed reconstruction of the stratigraphic architecture relying on lithofacies correlations of more than 900 boreholes and wells, and integrated with a geophysical survey based on the HVSR technique (Horizontal to Vertical Spectral Ratio) enables the identification of three depositional domains within the study area. Despite their common alluvial origin, the three domains exhibit distinct surface morphology and subsurface deposits stacking patterns, implying different geotechnical behaviours, as revealed by the comparison between the obtained subsurface geological model and the ground-subsidence maps derived from InSAR (Interferometric Synthetic Aperture Radar) data. The subsidence values, in fact, display a spatial distribution within the study area that allows the distinction of three different areas, well overlapping the three identified geological domains.

The present study emphasizes the effectiveness of the lithofacies approach in constructing a reliable geological model within complex alluvial settings, as the subsurface units are correlated considering the depositional environment they belong to and the inferred geometry, thus reducing the subjectivity of interpretation and providing useful information on potential geotechnical implications.

## **2. Study area**

The city of Bologna (Italy) is located at the southern margin of the Po Plain (Fig. 1). The Po Plain represents the surface of a subsiding foreland basin, bounded by two fold-and-thrust belts: the Alps to the north and the Northern Apennines to the south (Pieri & Groppi, 1981). This foreland basin is filled by a Pliocene–Quaternary sedimentary succession characterized by shallowing-upward sequences (Castellarin et al., 1985; Ricci Lucchi, 1986). Most of the Northern Apennines, including the areas south of Bologna, has undergone a general uplift since the early Pleistocene (Argnani et al., 2003). The Po Plain, instead, including the area of Bologna, subsided at rates of 1–2 mm/year during the last 1.43 million years (Carminati & Di Donato, 1999).

The study area is about 88 km<sup>2</sup> and extends west to east from the Reno River to the Savena River, and south to north from the Apennine foothills to the northern suburbs of Bologna (Fig. 1). Elevation ranges from about 80 m a.s.l. at the Apennine foothill to about 30 m above sea level (a.s.l.) in the northwest corner.

Surface deposits mostly consist of gravels, sands, and fine-grained soils related to the fluvial activity of the Reno and Savena rivers.

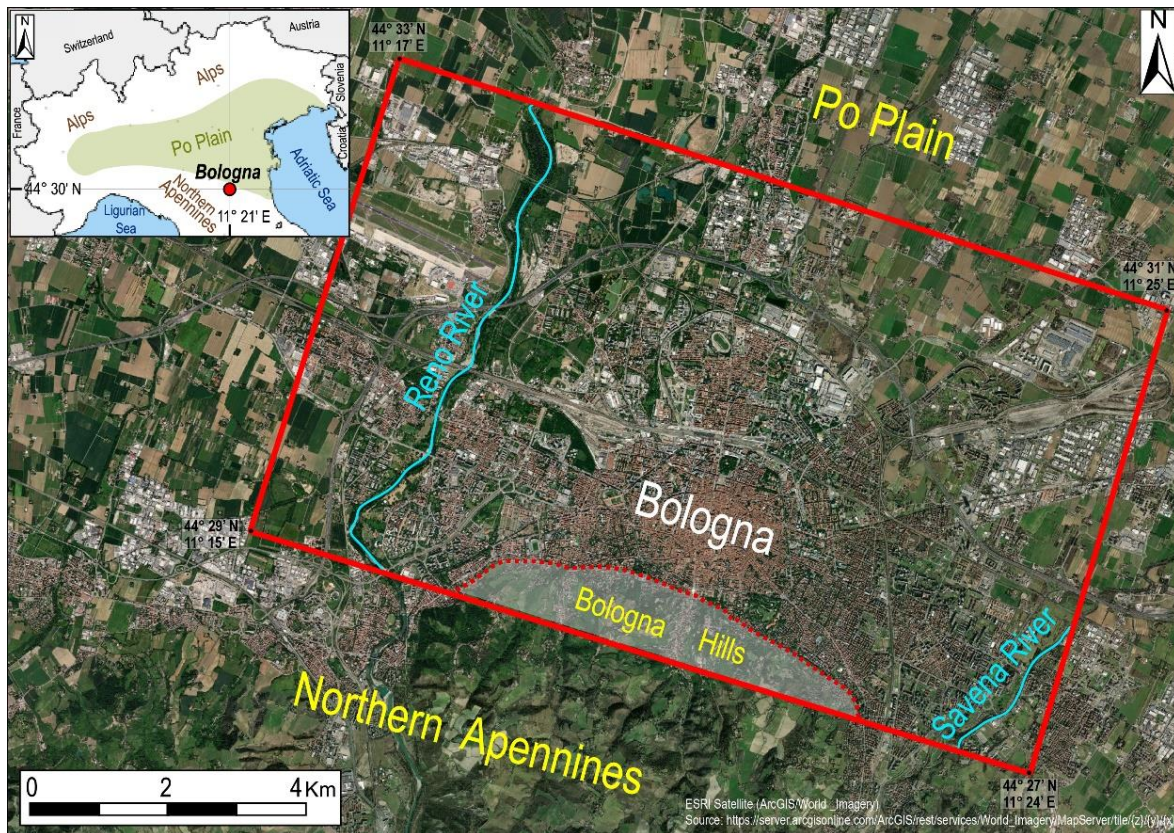


Figure 1- Study area

According to the Geological Map of Italy 1:50000 (Sheets 220, 221 and relative notes by the Geological Survey of Italy – ISPRA, Istituto Superiore per la Protezione e la Ricerca Ambientale), thick gravel bodies are present at the outlets of the Reno and Savena rivers, that grade into alternations of sands with mud-prone strata in their distal part (section AA', Fig. 2). Underneath the Bologna historical centre (see Fig. 2, section BB') coarse-grained fluvial deposits are rare and occur only at depths greater than 100 m. The centre of Bologna, indeed, acted as an interfluvium during the Holocene, the Late Pleistocene, and part of the Middle Pleistocene (Amorosi et al., 1996, 1997; Bruno et al., 2013). Here, a stacked succession of paleosols dating from the Middle Pleistocene onwards suggests prolonged periods of subaerial exposure (Amorosi et al., 2014; Bruno et al., 2020).

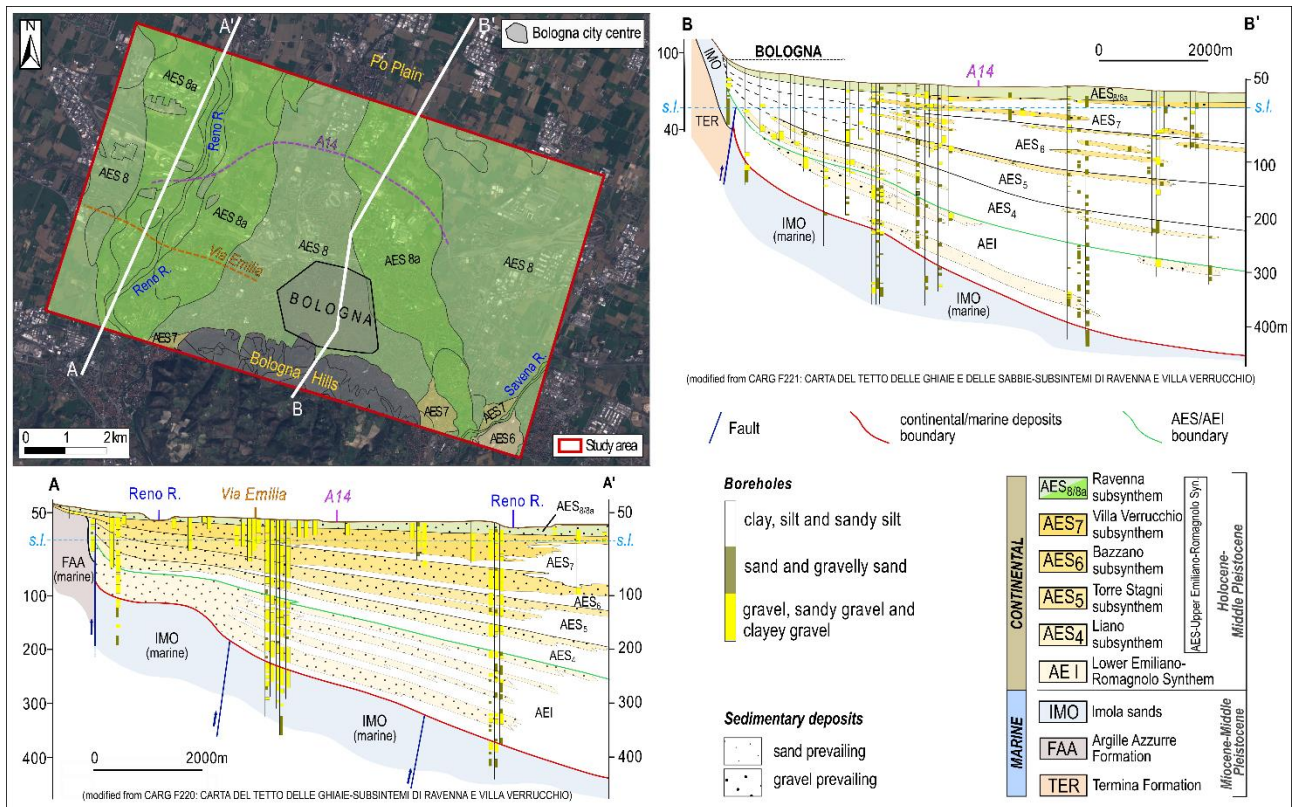


Figure 2- Geological setting of the study area. Geological map of Bologna and stratigraphic cross-sections showing the late Quaternary stratigraphy beneath the Reno River (AA') and the urban area of Bologna (BB'). In the Geological Map of Italy 1:50000 (Sheets 220-221 and related notes), alluvial deposits are subdivided into two synthems, the Lower and the Upper Emilia-Romagna Synthems (AEI and AES, respectively), separated by a regional unconformity dated to 450 ky BP (Martelli et al., 2017). The base of AEI is marked by the unconformity separating marine-coastal sediments (TER, FAA, and IMO) from continental deposits, dated to ca. 800 ky BP (Gunderson et al., 2014). The internal architecture of AEI and AES is characterized by the cyclic alternation of coarse-grained deposits with fine-grained strata (Amorosi et al., 1996; 2008), reflecting Milankovitch-scale (100 kyrs) climate oscillations. This cyclic structure of lithofacies permitted the subdivision of AES into five lower-rank units (subsynthems): AES<sub>4</sub>, AES<sub>5</sub>, AES<sub>6</sub>, AES<sub>7</sub>, and AES<sub>8</sub>. Sediments belonging to AES<sub>8</sub> (dated to the Holocene) and its sub-unit AES<sub>8a</sub>, corresponding to post-Roman deposits, are largely exposed in the study area.

### 3. Methodology



The 3D geological model of Bologna was developed by integrating surface and subsurface data as shown in Figure 3.

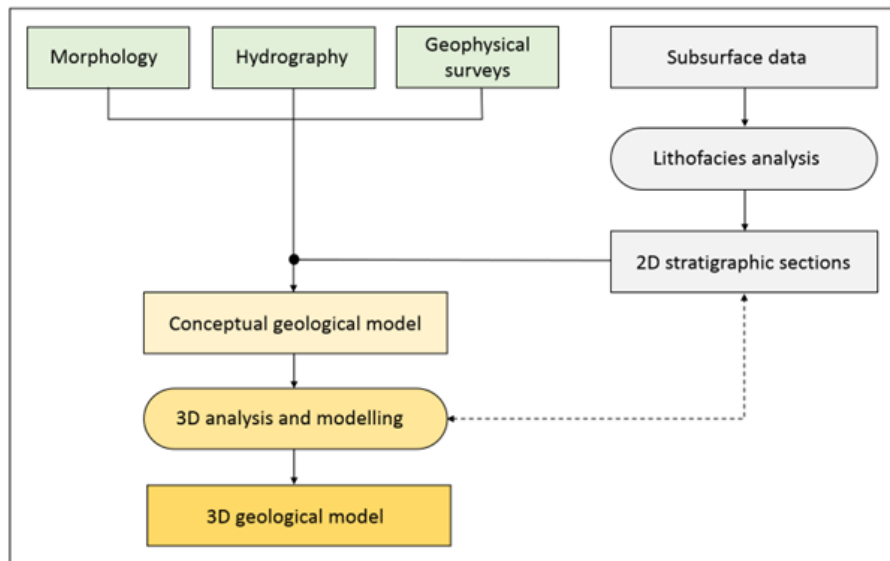


Figure 3- Flowchart illustrating the methodology employed to develop the 3D geological model of the study area. Rounded boxes highlight activities driven by expert judgment.

### 3.1 Surface morphology

Surface morphology was analysed using a 10 m resolution Digital Terrain Model (DTM) obtained by digitizing the contour lines from the 1:5000 topographic map. The DTM has a planimetric accuracy (Root Mean Square - RMS) of 4 m, and although small-scale fluvial landforms such as levees, terraces, or depositional lobes may not be discernible, the DTM effectively captures the overall topography of the area. To enhance the visibility of the main topographic features associated with fluvial activity, we employed a custom colourmap consisting of a repeated sequence of rainbow colours (see sect. 4.6). Additionally, a set of topographic profiles with varying orientations was extracted to highlight the main topographic changes.

### 3.2 Urban river network

The urban area of Bologna is fed by several small watercourses that flow down the hills and cross the city through a network of canals and sewage. These streams are characterised by small watersheds (a few square kilometres) with very limited sediment transport capacity. However, during the Holocene, they delivered large amounts of sediment to the area between the Reno and Savena rivers playing a significant

role in land building. The stream network of the urban area was reconstructed by integrating recent literature (Cremonini, 1980; 1992; Elmi et al., 1984) with historical maps (Chiesa, 1742).

### 3.3 Geophysical surveys

A geophysical campaign based on the HVSR technique (Horizontal to Vertical Spectral Ratio, Nakamura, 1989) was carried out to detect the boundary between marine and continental deposits (IMO-AEI limit in Fig. 2) and support the stratigraphic analysis. HVSR measurements provide an estimate of site resonant frequencies that are a function of subsurface geology (Castellaro & Mulargia, 2009; Choobbasti et al., 2013; Moisedi et al., 2015, Martona et al., 2016; Akkaya & Özvan, 2019). Forty-five HVSRs tests were performed in the central and southern parts of the city (Fig. 4) using a three-component sensor-velocimeter (Tromino™ from Micromed). To achieve adequate statistical sampling for the frequency range used in this study (0.1 to 64 Hz), ground vibrations were sampled at 128 Hz for 16 minutes at each measurement station (SESAME, 2004). HVSR data were then combined with the results of MASW (Multichannel Analysis of Surface Waves) and ESAC (Extended Spatial Autocorrelation) surveys carried out by the Geological, Soil and Seismic Survey of Emilia-Romagna (RER) as part of the seismic microzonation of Bologna, to assess the shear-wave velocity profile at each measurement station. Post-processing was undertaken using the Grilla software (Micromed).

### 3.4 Boreholes and wells

Subsurface stratigraphic data were extracted from the open-access RER geognostic database. The RER database returned 940 stratigraphic data consisting of 312 water wells and 628 continuous-core boreholes. The overall data density is about 10 points for km<sup>2</sup>, with a mostly clustered spatial distribution. The highest density is around railway lines and pumping well fields while the lower density is in the northern part of the area (Fig. 4). The major differences between wells and continuous cores are the quality of log descriptions and the investigation depths. Continuous cores are generally shorter but contain accurate lithological descriptions that are useful for facies interpretation. Water wells are typically deeper (down to 480 m, Fig. 4), but often subsurface stratigraphy is poorly described. The wide time span of the dataset (from 1900 to 2021) is a further element of complexity since the terminology and detail used for the stratigraphic description varied through time.

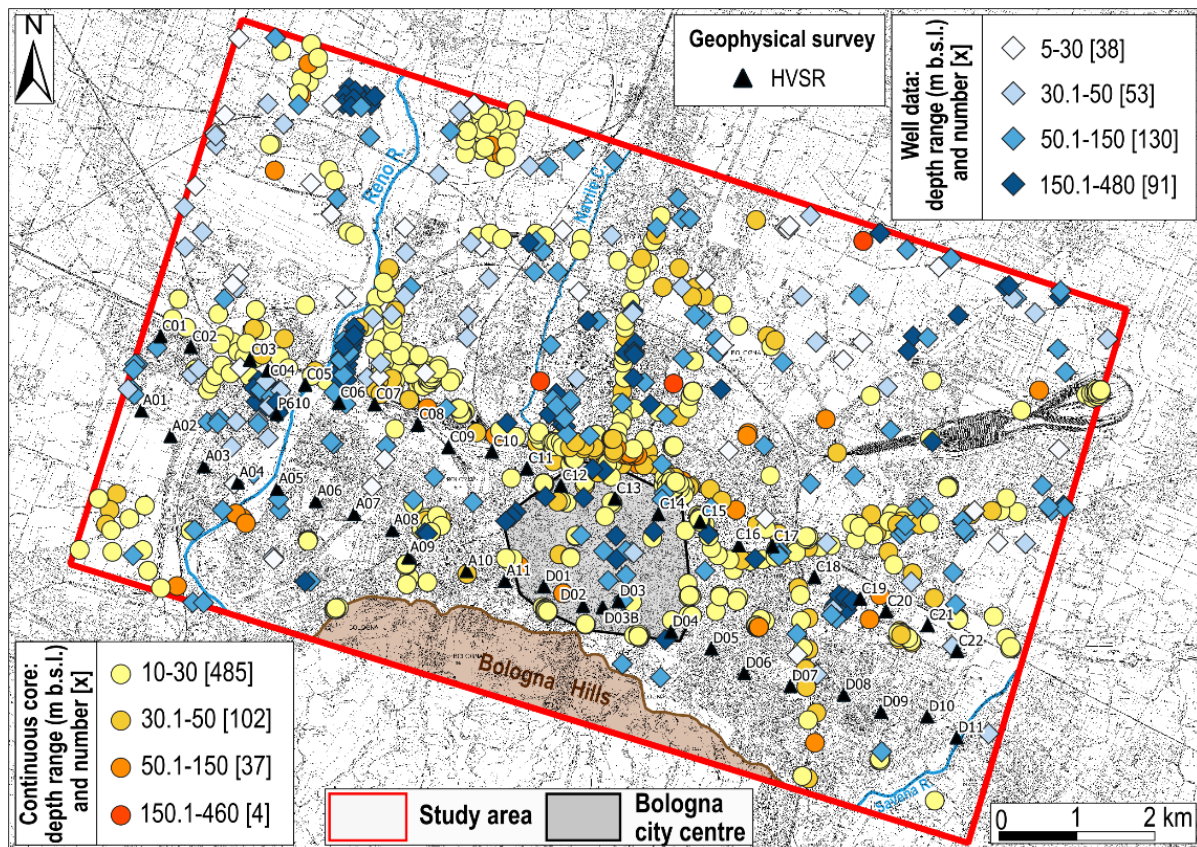


Figure 4- Subsurface data and geophysical investigations. Location of boreholes and wells extracted from the RER geognostic database (circles and diamonds) and HVSR measurements (triangles).

### 3.5 Lithofacies analysis

All the boreholes and wells were re-interpreted in terms of lithofacies. Lithofacies are stratigraphic intervals based on lithology and a set of accessory components (fossils, vegetal remains, carbonate nodules etc.) that bear a direct relationship to the depositional process. Lithofacies are the key component of facies associations, which are usually defined by the study of outcrops (where two- or three-dimension geometry and lateral extent of sediment bodies can be observed) and by analogy with modern depositional environments (Allen, 1963; Bridge et al., 2000). Stratigraphic correlations guided by lithofacies and their lateral relationships (facies tracts) allow a plausible reconstruction of subsurface stratigraphy, as they offer a reliable picture of sediment bodies and their geometry. In complex alluvial environments, such as the subsurface of Bologna, lithofacies analysis requires integrating basic geological information (grain size, texture, and thickness) with additional data, such as the type (abrupt vs gradual) of stratigraphic contact. Based on the existing literature on lithofacies of alluvial systems, both from worldwide outcrops (e.g.,

Miall, 1977, 1978, 1985) and exposures near Bologna (Ori, 1982; Bruno et al., 2015), nine different lithofacies, listed and described in Table 1, were considered. The lithofacies and their reciprocal spatial relationships are graphically depicted in Figure 5, where the two depositional environments that typically host such lithofacies, i.e., the alluvial fan and the alluvial plain, are schematically represented. As it can be seen, gravelly lithofacies characterise both alluvial fan and floodplain environments with different plan distribution and vertical stacking pattern due to the different sedimentation processes. Amalgamated successions of gravels with radial arrangements on plan dominate the proximal and medial portions of the alluvial fan (A-B, B-C, Fig. 5). These deposits result from the loss of flow capacity of a fluvial channel emerging from a mountain catchment onto the plain. In proximal locations gravels are typically very thick, massive and poorly sorted (lithofacies *PC*, Tab. 1). Moving towards the plain, these deposits (lithofacies *DC*, Fig. 5) may vertically alternate with fining-upwards sequences of gravelly and sandy deposits (lithofacies *Ch1*, Fig. 5). These alternations result from the irregular and intermittent activity of multiple channels characterising the medial portion of the alluvial fan. In distal portions (C-D, Fig. 5), where the channels activity become prevalent, lithofacies similar to those characterising the alluvial plain can be found. Fluvial channels are responsible for the alluvial plain formation. Fining upwards gravelly-to-sandy/silty deposits (lithofacies *Ch*, Tab. 1) typically mark the depocentral area of the river. In the adjacent areas, such as levees (lithofacies *Lv*, Tab. 1) and overbanks (lithofacies *O*, Tab. 1), increasing amount of silty, silty-clayey, and clayey deposits, with latero-vertical heteropy typically occur. Within these areas, sandy-to-silty layers (lithofacies *Cr*, Tab. 1) may also be present, whereas the floodplain (*PF/WF*) is dominated by clayey deposits.

Code	Lithofacies	Main sedimentological features
<i>A/S</i>	Anthropogenic/Soil	Surficial deposits made of heterogeneous filling material, such as brick fragments, pebbles, and asphalt often included within a matrix of variable grain size ( <i>A</i> ) or vegetal terrains frequently containing roots and organic matter ( <i>S</i> )
<i>PC/ DC</i>	Proximal alluvial fan channel/ Distal alluvial fan channel	Very thick hetero-granular and heterogeneous gravel deposits, from matrix-supported to grain-supported, with frequent amalgamation and usually abundant sandy/clayey matrix ( <i>PC</i> ) or very thick gravel deposits typically characterised by a clast-supported texture with a subordinate sandy/clayey matrix ( <i>DC</i> ).

<i>Ch</i>	Fluvial channel	Thick gravel-to-sand and coarse sand-to-silty sand deposits, typically forming fining-upward sequences, corresponding to the equivalent at distal location, i.e., towards the plain, of the gravel-rich facies identified at the river outlet ( <i>PC</i> and <i>DC</i> ) and mostly characterising the middle-distal portion of the plain.
<i>ChA/Dv</i>	Channel abandonment/ Deactivation	Clay, less frequently silt, with a very low average thickness, sharply lying on thick gravel deposits. At distal locations ( <i>ChA</i> ), clays may include organic matter, while at more proximal locations clays are associated with thin pebble or sand layers ( <i>Dv</i> ). <i>ChA</i> is interpreted as the abrupt abandonment of the fluvial channel, such as in the case of an avulsion event, and may pass upwards to the floodplain facies (e.g., <i>O</i> , <i>WF</i> , and <i>PF</i> ). <i>Dv</i> represents, instead, the sudden deactivation of a stream. It can be followed by reactivation, testified by the superposition of thick gravel deposits, corresponding to lithofacies <i>PC</i> and/or <i>DC</i> .
<i>Lv</i>	Levee	Alternating cm-thick to dm-thick silt/clay and sand deposits. This lithofacies usually characterises the upper part of a fluvial channel sequence, although it may be also found within a thick floodplain succession.
<i>Cr</i>	Crevasse	Thin fine sand to sandy silt deposits usually associated with flood layers formed when riverbanks break up, with the spilling of sandy and silty deposits on the floodplain. Crevasse deposits can interrupt floodplain sequences abruptly, at distinct stratigraphic levels.
<i>O</i>	Floodplain with overbank	Clay deposits of variable consistency and thickness, marked by the recurrence of thin silty, sandy silt, and silty sand layers. They represent the over-bank deposits, related to flood events affecting floodplain areas nearby the fluvial channel.
<i>WF</i>	Well-drained floodplain	Usually thick, yellowish to brownish, mostly stiff, clay deposits. The occurrence within clayey deposits of calcareous nodules is very common. This lithofacies represents undisturbed floodplain deposits, usually undergoing subaerial exposure
<i>PF</i>	Poorly-drained floodplain	Light to dark grey, generally soft clay, usually thick, occasionally including organic material. This lithofacies corresponds to undisturbed floodplain deposits, commonly undergoing stagnant conditions.

Table 1- Lithofacies used to characterize the alluvial deposits under the city of Bologna.

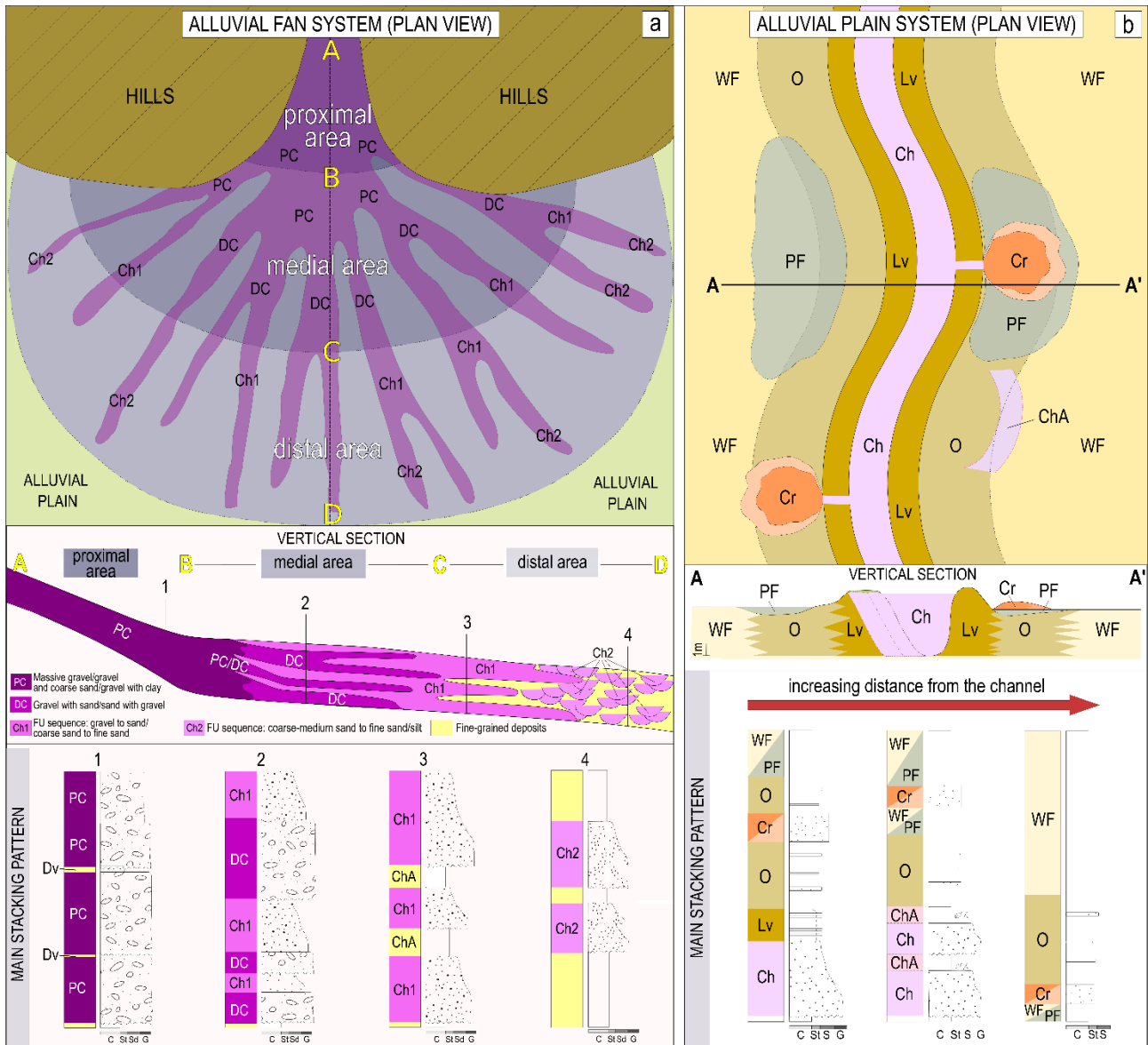


Figure 5- Depositional environments and lithofacies distribution. Schematic representation of an alluvial fan (a) and alluvial plain (b) depositional systems with the spatial locations of the corresponding different lithofacies.

### 3.6 Two-dimensional stratigraphic cross-sections

Thirteen stratigraphic cross-sections were drawn parallel and perpendicular to the general depositional strike to identify the main sedimentary bodies (Fig. 6). Eight cross-sections were traced NW-SE and five SSW-NNE, covering the whole study area. All transects were drawn to intercept the most significant boreholes, with a resulting average spacing of 1 borehole every 400 m. Along each section, stratigraphic correlations were carried out based on the lithofacies criterion illustrated in the previous section, overcoming the limitations arising from the oversimplified correlation of strata on a lithological basis.

Considering the expected geometry of each deposit type, similar lithofacies were correlated based on their stratigraphic position, essentially allowing the lateral and vertical distribution of fluvial deposits to be traced, as opposed to floodplain deposits (see sub-sect. 4.5.1 and 4.5.2). A denser grid of differently oriented straight-lined sections including projected boreholes data was then carried out within a 3D modelling software, Leapfrog Works (Seequent Limited) to validate the stratigraphic framework derived from the 13 main cross-sections shown in Figure 6.

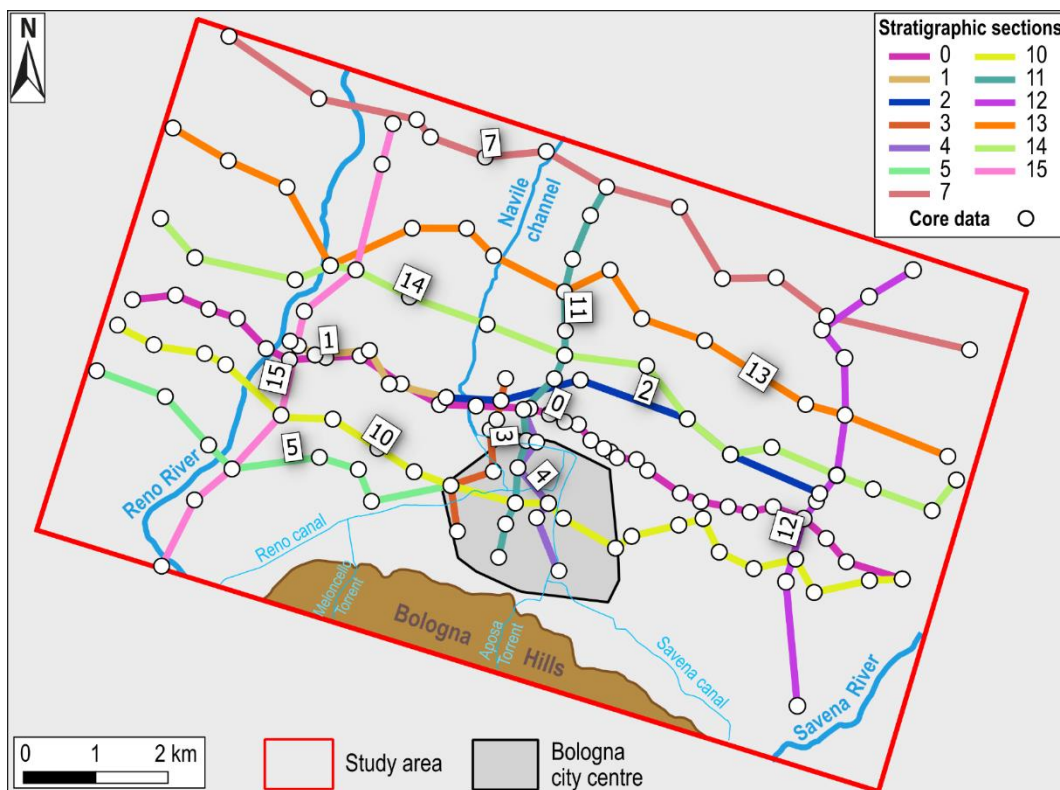


Figure 6- Location of the stratigraphic cross-sections.

### 3.7 Simplified geological model

The combination of surface morphology, drainage network, geophysical surveys, and 2D stratigraphic cross-sections lead to the development of a simplified geological model. In particular: *i*) surface morphology supported facies interpretation in the shallow subsurface based on core descriptions; *ii*) river network analysis guided the correlation of coarse fluvial deposits and possible subsurface distribution of ancient alluvial fan complexes (lithofacies *Ch*, *PC*, and *DC*); *iii*) geophysical surveys were used to model the boundary between continental and marine deposits detected in deep boreholes; *iv*) 2D stratigraphic

sections provided the geometry of the main sedimentary bodies. The simplified geological model provided a basic understanding of the main geological domains and guided 3D modelling in our complex case.

### 3.8 3D geological model

3D geological modelling was carried out using the Leapfrog Works 3.1 software. This software allows to visualise and manage spatial data and can model underground infrastructures like tunnels or pipelines, which are important in urban areas. The 940 boreholes selected from the RER database, reinterpreted in terms of lithofacies, were uploaded to the Leapfrog environment and the modelling domain volume was created. To outline the model within the three dimensions, the perimeter of the study area was used to define its lateral extent, whereas the DTM and the continental/marine boundary were chosen as its top and bottom, respectively. Then, alluvial bodies were modelled according to the thirteen 2D stratigraphic cross-sections.

The 3D modelling was performed using two different interpolating tools, called “Intrusion” and “Deposit”. The two interpolators utilize distinct logic, algorithms and different operational procedures, producing alternative graphical outputs. The “Intrusion” tool generates a 3D surface that tightly encloses manually selected lithofacies intervals from a restricted group of boreholes, resulting in a limited extension sedimentary body. This 3D surface interpolation is based on a linear semi-variogram model, which assigns weight to the surrounding stratigraphic data based on their distance from the considered deposit (Seequent, 2019). The “Deposit” tool interpolates a sheet-like surface that passes through the contact points between two distinct units, based on their stratigraphic relationships, in terms of “younger/older” deposits. This surface considers/include all the available boreholes, extending to the whole modelling domain, and represents the top/bottom of a certain unit with respect to a confining one. Thus, two surfaces (i.e., top and bottom) are needed to /define each single tabular sedimentary body. In both scenarios, the modelling procedure for each element is manually controlled and based on the attribution of user-defined parameters describing its spatial orientation and shape. 3D modelling of our complex lithostratigraphic setting required a simplified operational approach. The logic was to merge lithofacies belonging to the same depositional environment: lithofacies *Ch*, *PC*, *DC*, *Lv*, *Cr*, *ChA/Dv*, and *O*, which refer to the fluvial environment in which traction processes prevail, were grouped and attributed to a single class named “granular deposits”;



whereas *WF* and *PF*, related to the fluvial environment dominated by the settling of clay particles, were grouped in a single class named “fine-grained deposits”. Thin (<5 m) granular bodies embedded within thick fine-grained successions with low correlation potential were individually shaped with the “Intrusion” tool, but finally merged with the hosting fine-grained deposits and attributed to a third class named “fine-prevailing deposits”. Although the final model contains only three units (granular deposits, fine-grained deposits, and fine-prevailing deposits), all nine lithofacies were used to guide the correlation process.

## 4. Results

### 4.1 Surface morphology

The visual analysis of the DTM reveals a particular morphology for the study area. Although the topography is almost flat (Fig. 7a), three distinct zones were recognized (Fig. 7b):

- zone A is crossed by the Reno River and is characterised by an overall flat morphology, with relatively low ground elevation ranging between 30 and 50 m;
- zone B covers the urban area of Bologna and it is characterised by a slightly convex-up morphology, with a higher elevation of about 60 m;
- zone C is crossed by the Savena River and shows a marked convex-up morphology, with an average elevation of about 50-60 m.

Zone B, therefore, stands as a “relative high” between the Reno and Savena rivers. The transition from the Reno River (zone A) to the “relative high” is quite abrupt (see Fig. 7, topographic profile T1), while the western limit of the Savena River (zone C) is marked by a narrow incision. The “relative high” of the Bologna urban area is no longer present at a distal location (see topographic profile T2, Fig. 7) where areas A and C merge.

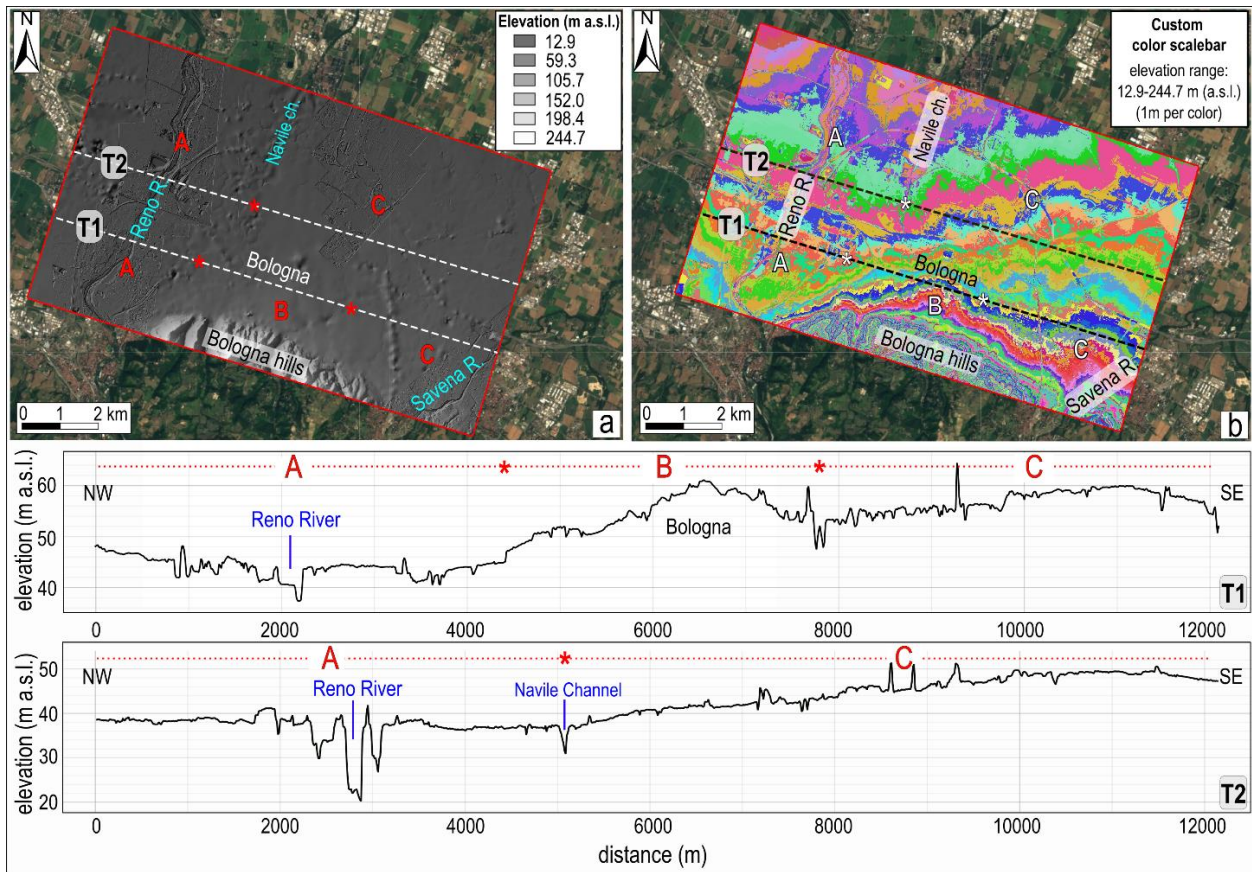


Figure 7- Shaded relief (a) and Digital Terrain Model (b) of the study area. T1 and T2 are topographic profiles showing the overall surface morphology perpendicular to the main depositional strike. The occurrence of local spikes along the two topographic profiles can be attributed to anthropic features (e.g., highways, overpasses...) and to artifacts depending on the quality of the DTM.

#### 4.2 Urban rivers network

Figure 8 shows the river network of the Bologna urban area. The streams flow in the south-north direction and cross the historical city centre merging with an artificial channel network dating back to the Middle Ages and Renaissance.

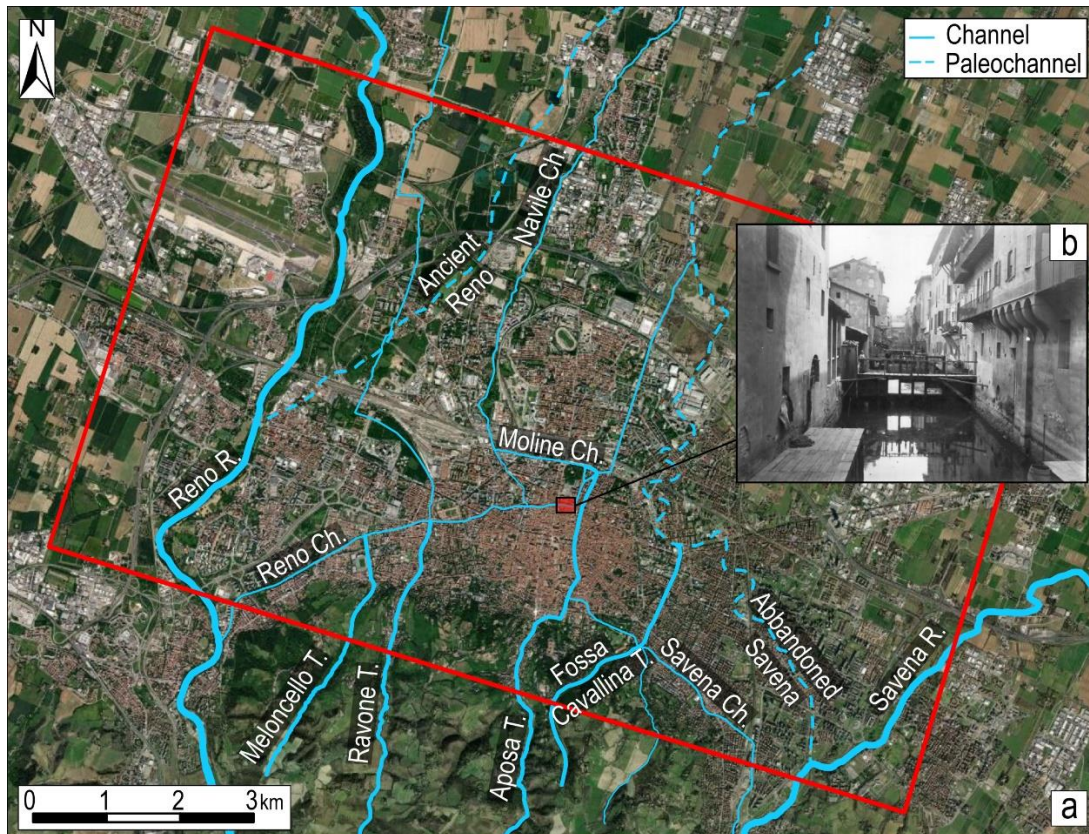


Figure 8- a) Hydrographic network of the study area. The thickness of the light-blue lines represents the type of channel: maximum for rivers, medium for torrents, and minimum for artificial canals. Dashed lines indicate paleochannels; b) the red square marks the location of the provided picture, showing a detailed view of the Moline channel (“Bologna, Moline Channel, Anonymous [1900-1920], Fondo Gonni”).

Within the perimeter of the historical centre, these artificial watercourses have a total length of about 6.6 km and nowadays, after centuries of human intervention, are buried for about 95% of their cumulative course. The sections that have not been filled mostly belong to the Reno and Moline channels (Fig. 8b). The anthropic channel network in the historical centre is fed by two artificial canals that depart from the Reno and Savena rivers. The first one, called Reno Canal, has a length of about 4.3 km and WSW-ENE orientation; the Savena Canal, is about 3.7 km long and ESE-WNW oriented. The other main artificial canal is the Navile, which flows for 4.6 km within the study area in a depressed reach elongated in SSW-NNE direction (possibly corresponding to a former Aposa riverbed, Elmi et al., 1984), located north of the city centre and about 3 km east of the Reno River. This zone and its prosecution northwards have been occupied during Roman times by a Reno River paleochannel, known as “Ancient Reno”. The Savena River historic course observed in historical maps (“Abandoned Savena” in Fig. 8a; Chiesa, 1742) was active until

1776, before diversion by anthropic activities (Cremonini, 1980; Elmi et al., 1984). Nowadays, the Abandoned Savena is fed by the anthropic channel network and is pensile in its northernmost section.

### 4.3 Geophysical surveys

The seismic stratigraphy obtained by HVSR measurements showed a good correlation with the 3 zones detected by surface morphology (A, B, C in Fig. 7). In zones A and C, several H/V peaks are present at shallow depth (see peaks identified by black arrows in Fig. 9 with values of approximately 10 Hz, likely related to the occurrence of gravel bodies interbedded with finer material), and shear waves velocity reach 600 m/s within the uppermost 50 m of depth (Fig. 9). Instead, in the Bologna urban area (zone B), a substantial homogeneity in the H/V trend is observed, and shear wave velocities reach 600 m/s only at depths greater than 150 m (Fig. 9).

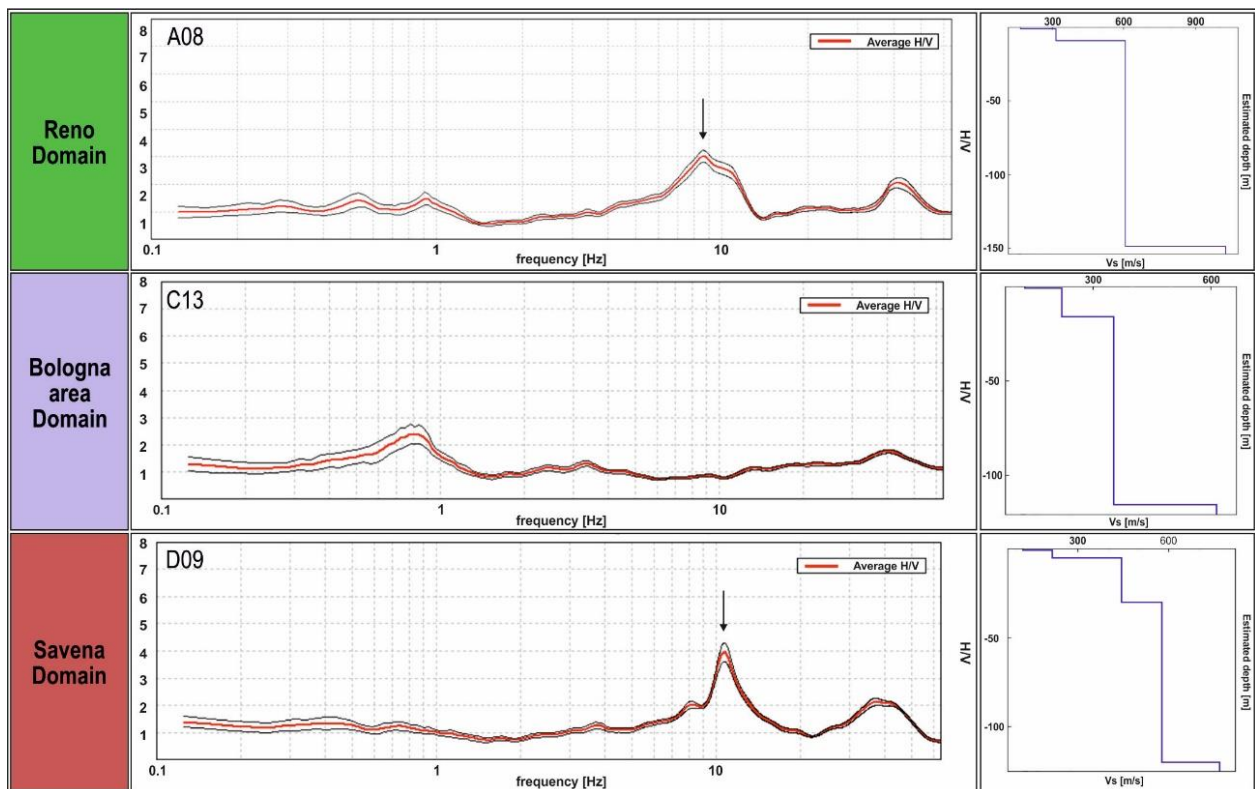


Figure 9- HVSR (Horizontal to Vertical Spectral Ratio) patterns. Comparison of HVSR measured in the three different domains. The figure includes H/V graphs and Vs models resulting from the processed measurements. The H/V graphs and Vs variations with depth show similar patterns for the Reno and Savena areas (zones A and C, sub-sect. 4.1) significantly different from the pattern characterising the Bologna urban area (zone B, sub-sect. 4.1). Black arrows highlight H/V peaks likely related to gravel bodies interbedded with finer material.

The boundary between Quaternary continental and marine deposits was clearly detected only in 11 of the 35 HVSR measurements (Table 2). Here, an abrupt change in shear wave velocity was observed at a depth consistent with the continental/marine transition reported in the literature (RER & ENI-AGIP, 1998). In all other instances, the increase in shear wave velocity is considered as small or uncertain, likely because of the small difference in seismic impedance between the two sequences of deposits.

HVSR measurement	Domain	Elevation (m a.s.l.)	continental/marine boundary		Vs (m/s)
			Depth (m)	Elevation (m a.s.l.)	
A04	A	42.6	244.6	-202	955
A08	A	47.2	149	-101.8	606
A09	A	53.3	145.5	-92.2	535
A10	A	56	161.5	-105.5	603
A11	A	61.9	158.5	-96.6	542
C09	A	47.7	218.2	-170.5	683
C20	C	57.3	223	-165.7	541
C21	C	57.4	221.5	-164.1	530
C22	C	58.7	168	-109.3	508
D05	C	67	216	-149	655
D11	C	63.6	235.5	-171.9	590

Table 2- HVSR measurements. Lithofacies characterizing the subsurface of the study area: main sedimentary characteristics.

#### 4.4 Lithofacies analysis

The analysis of subsurface data in terms of lithofacies produced 940 tables, where distinctive lithofacies were assigned to each stratigraphic layer described in the borehole logs. Table 3 (Supplementary Material) shows, as an example, the lithofacies interpretation of the boreholes used in cross-section 10, which intersects the three morphological zones parallel to the foothills (Fig. 6). The lithofacies can be correlated both in the vertical (depth) and in the horizontal (planimetric) direction. An example of the planimetric lithofacies distribution for the shallow subsurface is shown in Figure 10. For each borehole, the prevailing lithofacies within the stratigraphic interval of 0-30 m is depicted in different colours. The resulting lithofacies pattern highlights a clear variation in the southern portion of the study area, from NW to SE, with proximal/distal alluvial fan channels in the Reno River area that pass to floodplains nearby the city of

Bologna, and again to proximal/distal alluvial fan channels towards the Savena River. A change in lithofacies can be also observed in the NW-SE direction along the Navile Channel, from proximal/distal alluvial fan channels to fluvial channels and floodplain deposits.

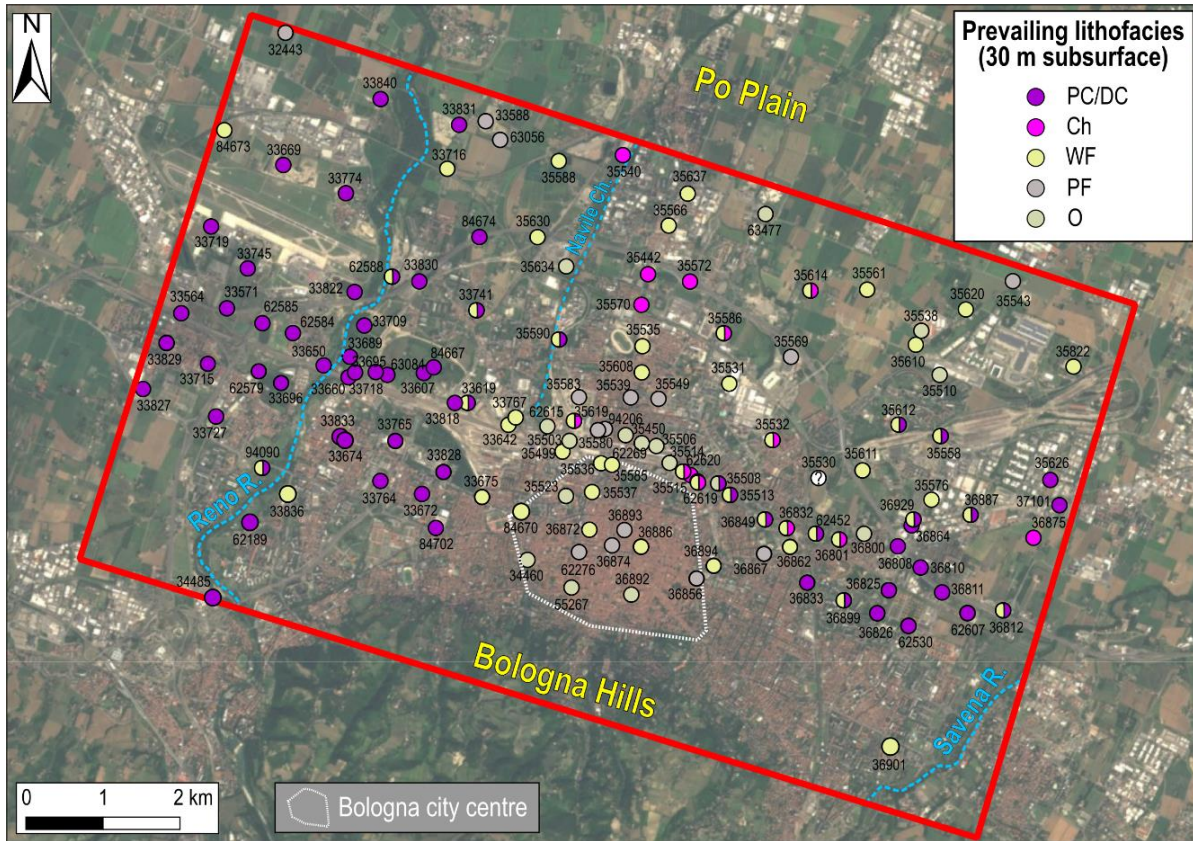


Figure 10- Example of subsurface data interpretation. Boreholes intercepted by the 13 main stratigraphic cross-sections, illustrating the different prevailing lithofacies characterizing the shallow subsurface (30 m). PC= proximal channel; DC= distal channel; Ch= fluvial channel; WF= well-drained floodplain; PF= poorly-drained floodplain; O= overbank.

Figure 11 provides a detailed depiction of the Savena River (zone C). Here, the lithofacies distribution is particularly complex and more data (detailed lithostratigraphic descriptions and surface hydrographic network) must be used to reduce subjectivity. As can be seen, a general S-N trend can be recognised, with lithofacies passing from proximal-to-distal alluvial fan channels to fluvial channels and floodplains. In the southern-central part, the planimetric lithofacies distribution is then combined with (i) information on the thickness and degree of amalgamation of coarse-grained deposits, and (ii) the main recent drainage axes, to reconstruct the different sedimentary bodies, highlighting the approximately radial trend consistent with an alluvial fan environment.

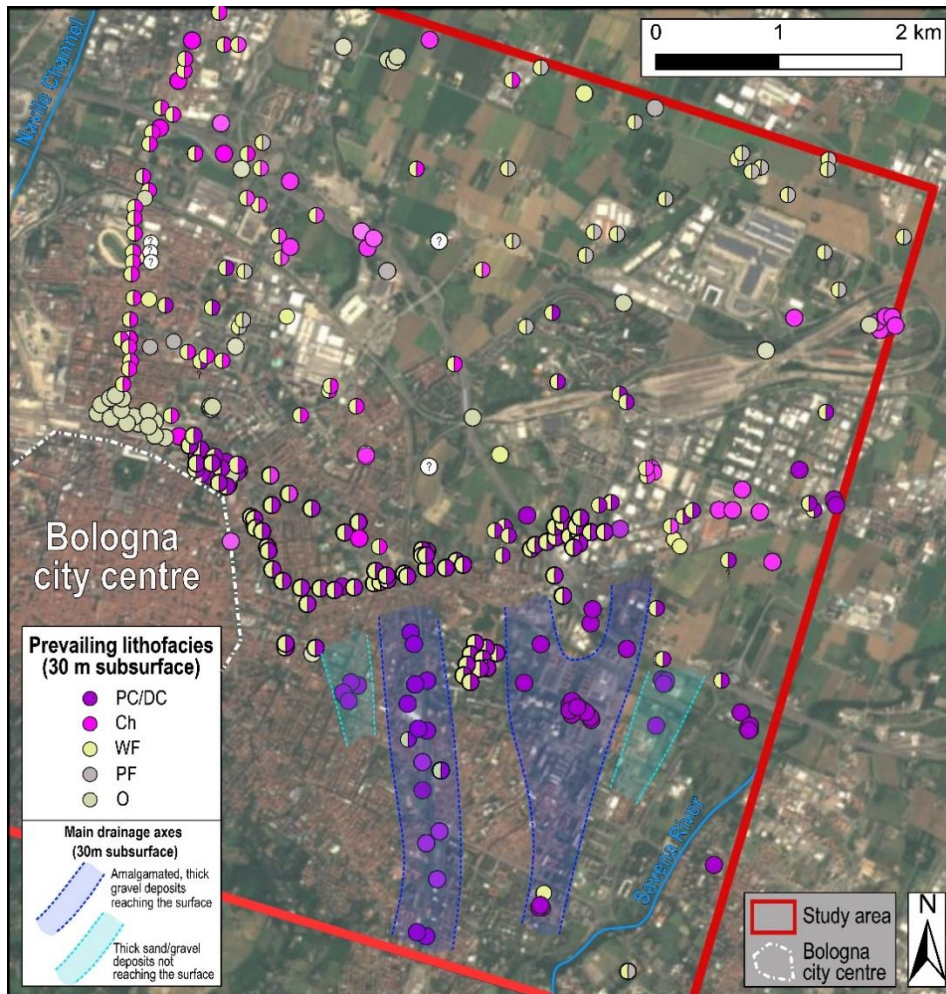


Figure 11- Detail of the Savena River area and plan lithofacies distribution. This zoomed-in view of the Savena River area illustrates the prevailing lithofacies within the shallow subsurface (0-30m) from the boreholes database. PC= proximal channel; DC= distal channel; Ch= fluvial channel; WF= well-drained floodplain; PF= poorly-drained floodplain; O= overbank.

#### 4.5 Two-dimensional stratigraphic cross-sections

Lithofacies were correlated in the subsurface across the thirteen 2D stratigraphic cross-sections shown in Fig. 6. Due to the varying depths of the boreholes and their uneven spatial distribution, the correlation is quite robust in the uppermost 100-150 m and more uncertain at depths exceeding 150 m. Despite these limitations and the inherent complexity of the alluvial environment, the stratigraphic sections revealed a well-defined stratigraphic framework.

##### *4.5.1 Transversal stratigraphic sections*

Figure 12 shows the two most significant sections drawn perpendicular to the main depositional strike. Section PP' crosses the proximal area parallel to the foothills and exhibits, from west to east, three

distinct depositional domains characterized by different fluvial-channel stacking patterns. The western part, corresponding to the Reno River domain, is characterised by two gravel-dominated stratigraphic intervals (*PC/DC*) 100-150 m thick (from the surface to about -80 m, and from about -110 m to -260 m respectively) separated by 20-30 m of fine-grained deposits (*WF*). The central part of the cross-section, which corresponds to the Bologna city centre, is marked by a 100-150 m thick mud-prone succession (*WF/PF*), with isolated gravel or sand bodies (a few m thick) mainly found at depths greater than 100 m (*Ch*). The eastern part of the cross-section corresponds to the Savena River domain and shows, again, the predominance of sand and gravel deposits (*PC/DC*) down to a depth of about 100 m. Gravel bodies are here thinner, less continuous and amalgamated than in the Reno domain.



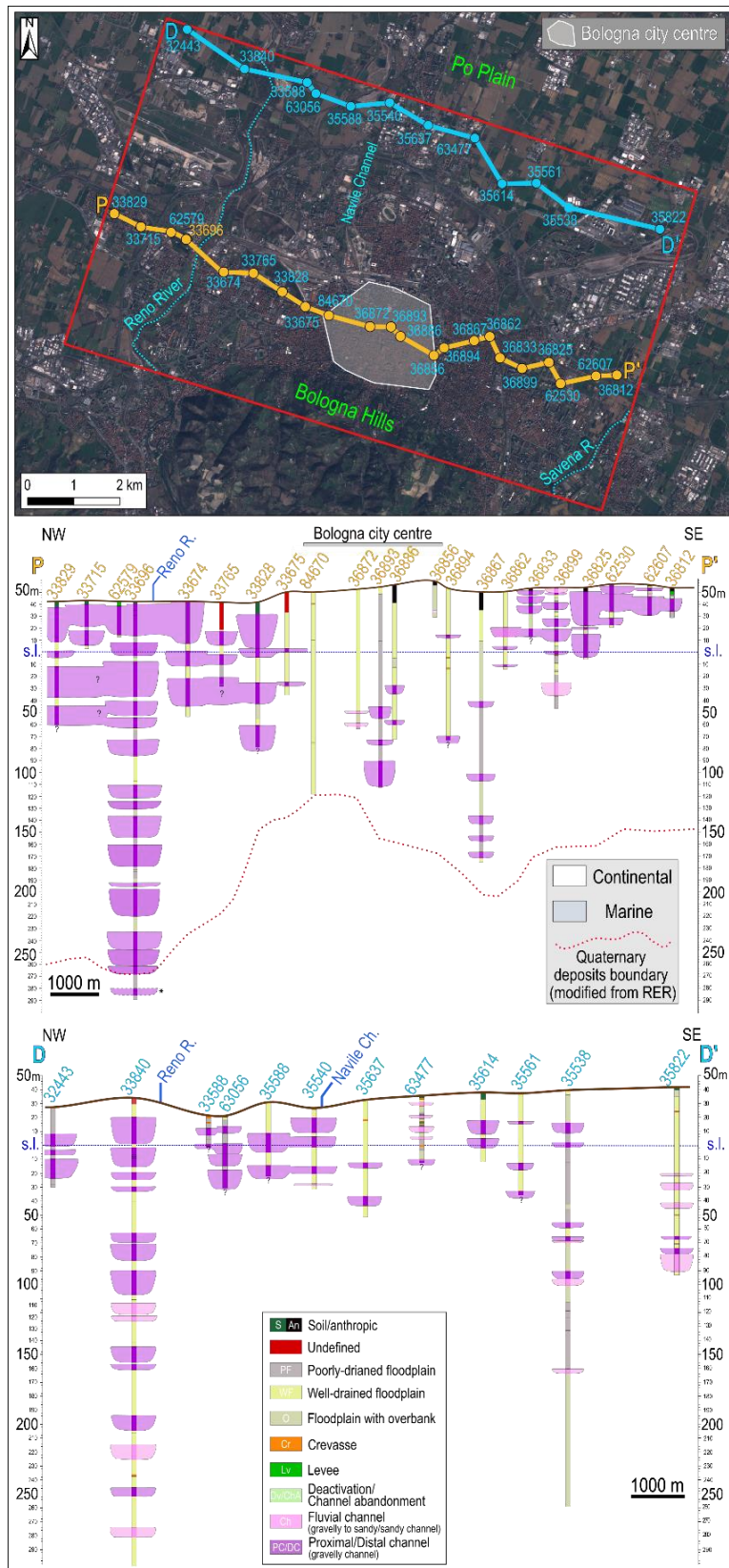


Figure 12- Transversal stratigraphic cross-sections: Proximal (PP') and distal (DD') intersecting the study area perpendicular to the main depositional strike. \*The deepest layer from the 33696 well stratigraphic log was interpreted as a channel deposit on the basis of a description that did not allow its attribution to a marine environment.

In a more distal position (section DD', Fig. 12), clay soils (WF/PF) are more abundant and two different stacking patterns of fluvial-channel deposits (*Ch*) can be observed: the western part is marked by alternating thick coarse-grained bodies with silt and clay, whereas the eastern sector is dominated by fine-grained deposits, with scattered sand or gravel bodies, a few metres thick.

#### 4.5.2 Longitudinal stratigraphic sections

Figure 13 shows three cross-sections drawn along the main depositional strike. Section RR' is along the Reno River and shows two massive gravel layers (*PC/DC*), 100-150 m thick, separated by a layer of fine-grained material about 20 m thick (*WF*). The vertical amalgamation of gravel bodies slightly decreases with depth (i.e., beyond about 100 m depth), with a parallel increase in the thickness of fine-grained deposits and the local occurrence of sand bodies a few metres thick. The central cross-section through the Bologna city centre (section MM') is dominated to the south by clay soils (*WF/PF*) with the occurrence, below about 100 m depth, of scattered, thin sand and gravel bodies (*Ch*). Northwards, the frequency of coarse deposits increases. The easternmost cross-section, drawn approximately along the Savena River (section SS', Fig. 13) shows a 50 m-thick succession of gravel bodies in the uppermost portion of the proximal area (*DC/PC*), which grades downsection into a clay-dominated succession (*WF/PF*) with sparse gravel and sand bodies (*Ch*), generally less than 10 m thick.

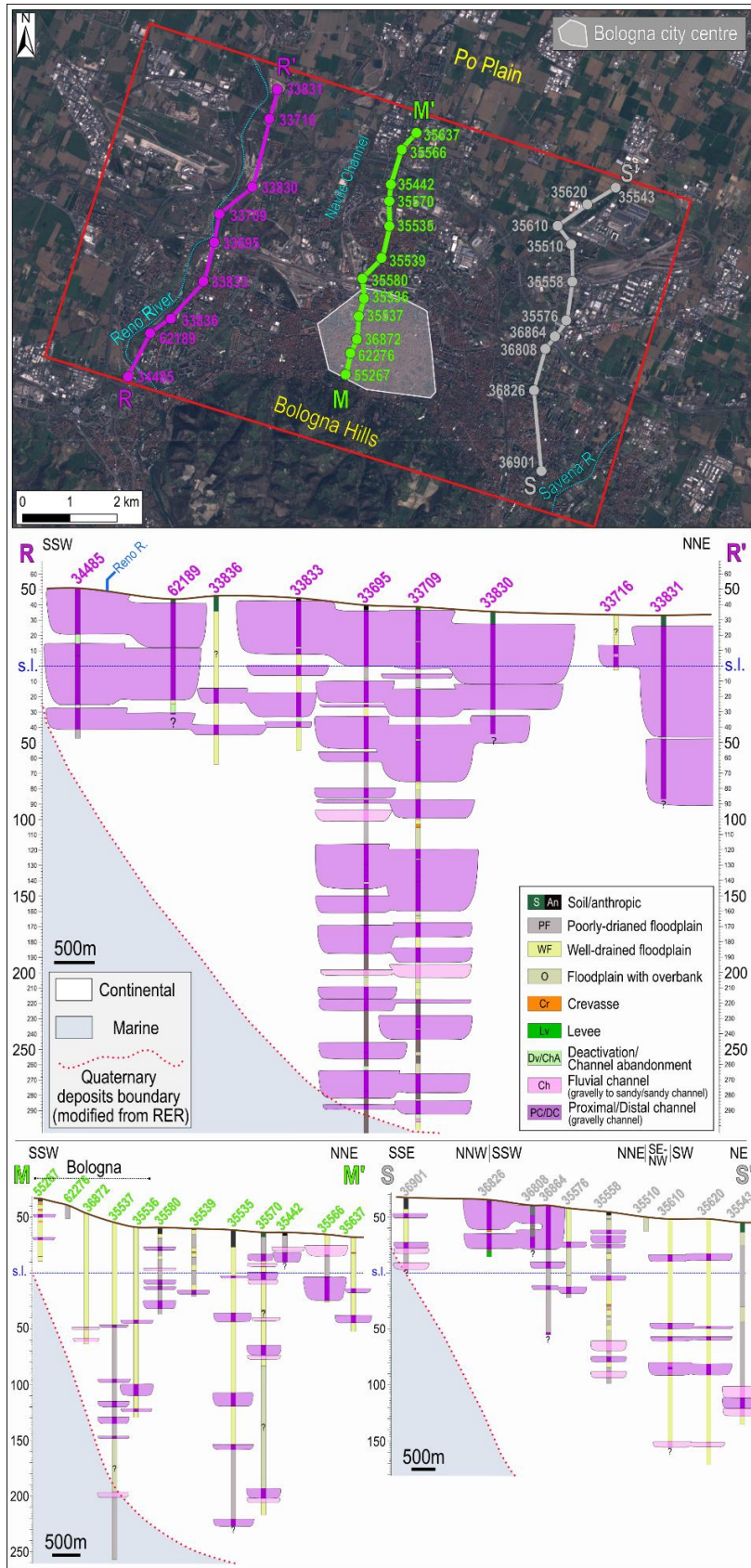


Figure 13- Longitudinal stratigraphic cross-sections Aligned parallel to the main depositional strike, intersecting the western (RR'), central (MM'), and eastern (SS') part of the study area.

#### 4.6 Simplified geological model

Morphological, hydrological, geophysical, and stratigraphic data were combined to obtain a simplified geological model of the study area. The first and most important outcome of data integration is the general agreement between surface morphology and subsurface depositional patterns. The three morphological domains identified through surface analysis (i.e., Domain A- Reno River; Domain B- Bologna historical centre; Domain C- Savena River) align with the three stratigraphic domains highlighted in cross-sections (Fig. 14). These domains also showed slight differences in the HVSR patterns detected during the geophysical survey (see Fig. 9, sect. 4.3). Domain A (Reno River) is the gravel-dominated filling of a river valley. The high degree of amalgamation of the channel bodies, as well as the abrupt transition with Domain B, suggest that the valley was partially confined to the east. Domain B (Bologna urban area) represents a morphological and stratigraphical divide, topographically elevated compared to the surroundings. This area is characterized by fine-grained deposits with frequent paleosols (Amorosi et al, 2014; Bruno et al., 2020). Domain C (Savena River) corresponds to a typical alluvial fan marked by a gentle convex-up surface morphology. The lower degree of lateral amalgamation of fluvial channel bodies reflects multiple events of nodal avulsion in the fan apex.

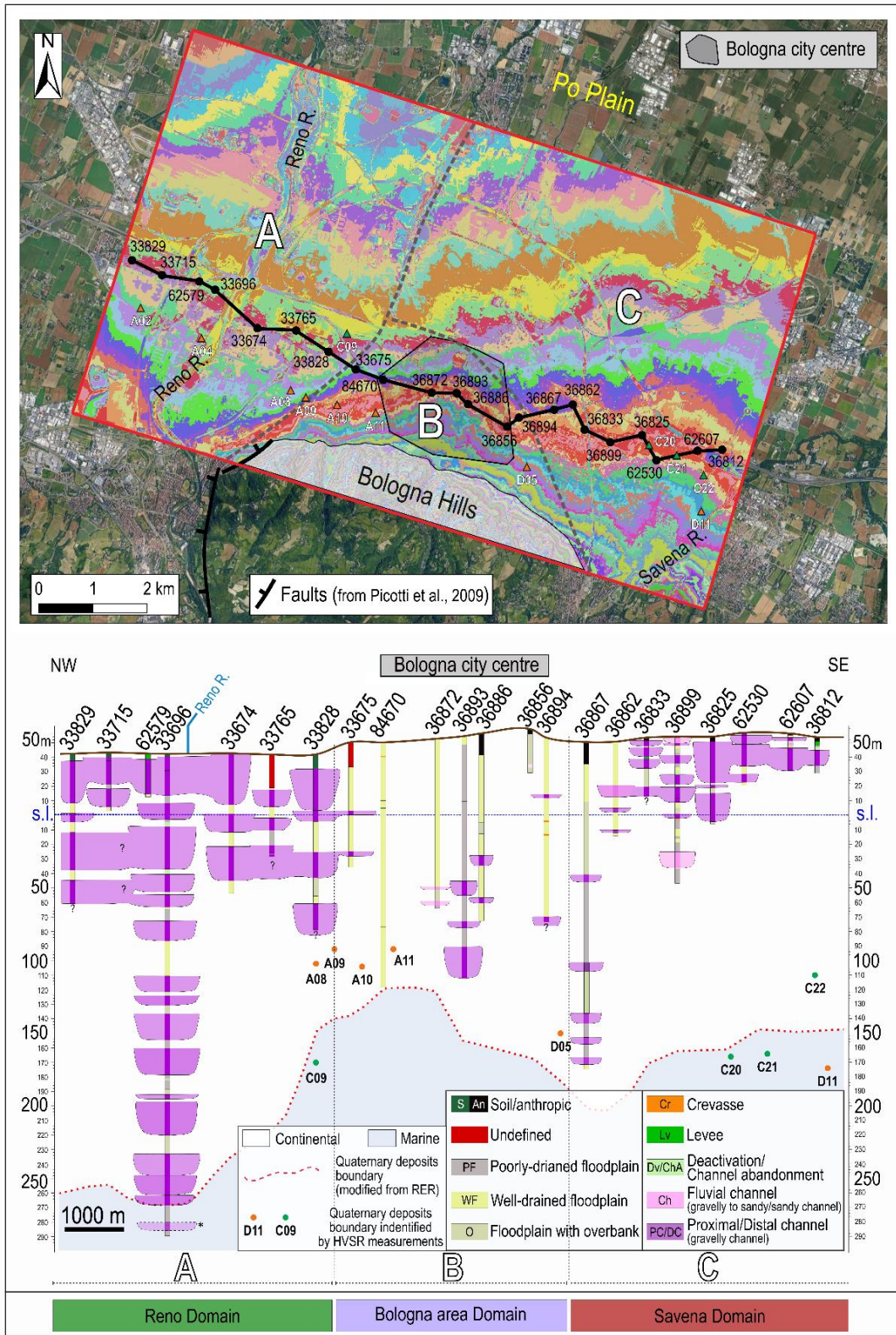


Figure 14- Simplified geological model of the study area. Upper) DTM plan view showing the three domains with distinct morphological characteristics (A, B, and C). Lower) Transversal stratigraphic cross-section highlighting the different stacking patterns observed in the three domains. HVSr measurements detecting the Quaternary continental/marine deposits boundary are also included. \*The deepest layer from the 33696 well stratigraphic log was interpreted as a channel deposit on the basis of a description that did not allow its attribution to a marine environment.

#### 4.7 3D geological model

The 3D geological model covers an area of 88 km<sup>2</sup> and extends to a maximum depth of about 400 m. According to the simplified geological model, the model bounding volume was subdivided into three sub-volumes corresponding to Domains A, B, and C (Fig. 15), bounded by two curvilinear surfaces. In section 4.5, it was observed that these surfaces denote transitional areas between distinct depositional domains rather than abrupt geological boundaries. Thus, they were positioned based on significant shifts in subsurface depositional patterns and surface topography.

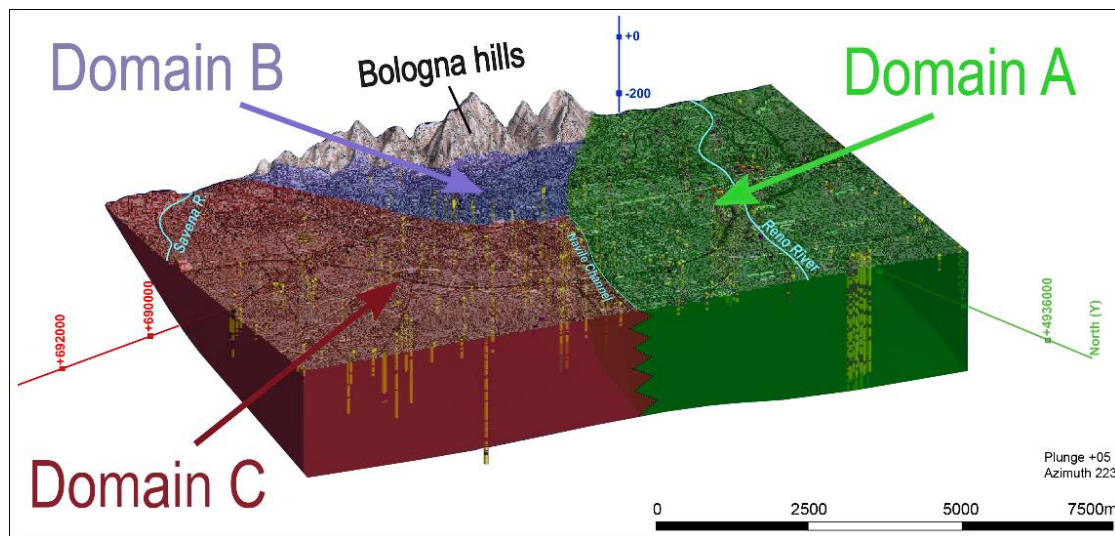


Figure 15- 3D view of the study area, displaying the distinction of the three geological domains. From east to west: the Savena alluvial fan (red block-Domain C), the Bologna relief (purple block-Domain B), and the Reno River (green block-Domain A).

A sub-vertical surface, dipping northwest, separates Domains A from B and A from C. This surface extends in a SW-NE direction west of the city centre (A-B boundary), and N-S along the Navile Channel (B-C boundary) (see Fig. 15). A second surface, dipping towards the plain with a slightly lower angle with respect to the previous one, separates domains A and C in the eastern part of Bologna. An additional, high-angle surface was added to exclude the Apennines from the model (Bologna hills in Fig. 15). Both coarse and fine-grained deposits were modelled in Domains A and C (Reno and Savena rivers), whereas in Domain B (Bologna city centre) only fine-grained deposits were considered.

In Domain C, granular soils were modelled following a conservative approach using the "Intrusions" tool (see sect. 3.8), because of the poor correlation potential of gravel and sand bodies supplied by the Savena

River. The “Intrusion” tool proved to be particularly effective in such an unpredictable context, where granular bodies show a spatial distribution and lithostratigraphic patterns consistent with the characteristics of an alluvial fan. In the proximal portion, in fact, the granular deposits are closely stacked and locally amalgamated, resulting in an almost single thick body, while in the middle-distal portion they are separated by fine-grained intervals and tend to be elongated on the horizontal plane following different orientations (Fig. 16a, b). The distal part of this domain is highly uncertain due to the uneven data distribution and the difficulty of carrying out lithostratigraphic correlations among scattered granular bodies. Here, a further sub-volume was used to indicate a thick sequence of predominant fine-grained deposits with dispersed granular layers (see Fig. 16a, b, “SRD fine-grained prevailing”).

In Domain A, the high lateral continuity of the granular bodies and the large number of boreholes allowed considering a double approach to model granular bodies, using both the “Intrusion” and “Deposit” interpolation tools, and thus obtaining two alternative geological models (Fig. 16a, b). Regardless of the interpolator used, the modelled granular bodies show a large areal extent at all stratigraphic levels and a high degree of amalgamation close to the mouth of the Reno River, where they tend to form a single thick body (from 100 m to more than 200 m depth). Towards the plain, the degree of amalgamation gradually decreases, and the granular layers (around 100-150 m thick) are separated by comparatively thinner layers of fine-grained deposits. Here, the different interpolation techniques provide quite different results: the “Intrusion” tool limits the extent of the granular bodies to a small volume around the stratigraphic data (Fig. 16a); the “Deposit” tool extends the interpolated volume to almost the entire domain (Fig. 16b). The NE part in the “Intrusion” model (Fig. 16a) is indicated as a “no-data” volume because this algorithm gives unrealistic results without stratigraphic data. Domain B (Bologna city) is characterised by the prevalence of fine-grained deposits. The occurrence of scattered granular bodies at great depth is maintained within the different stratigraphic logs, but not modelled as 3D volumes.

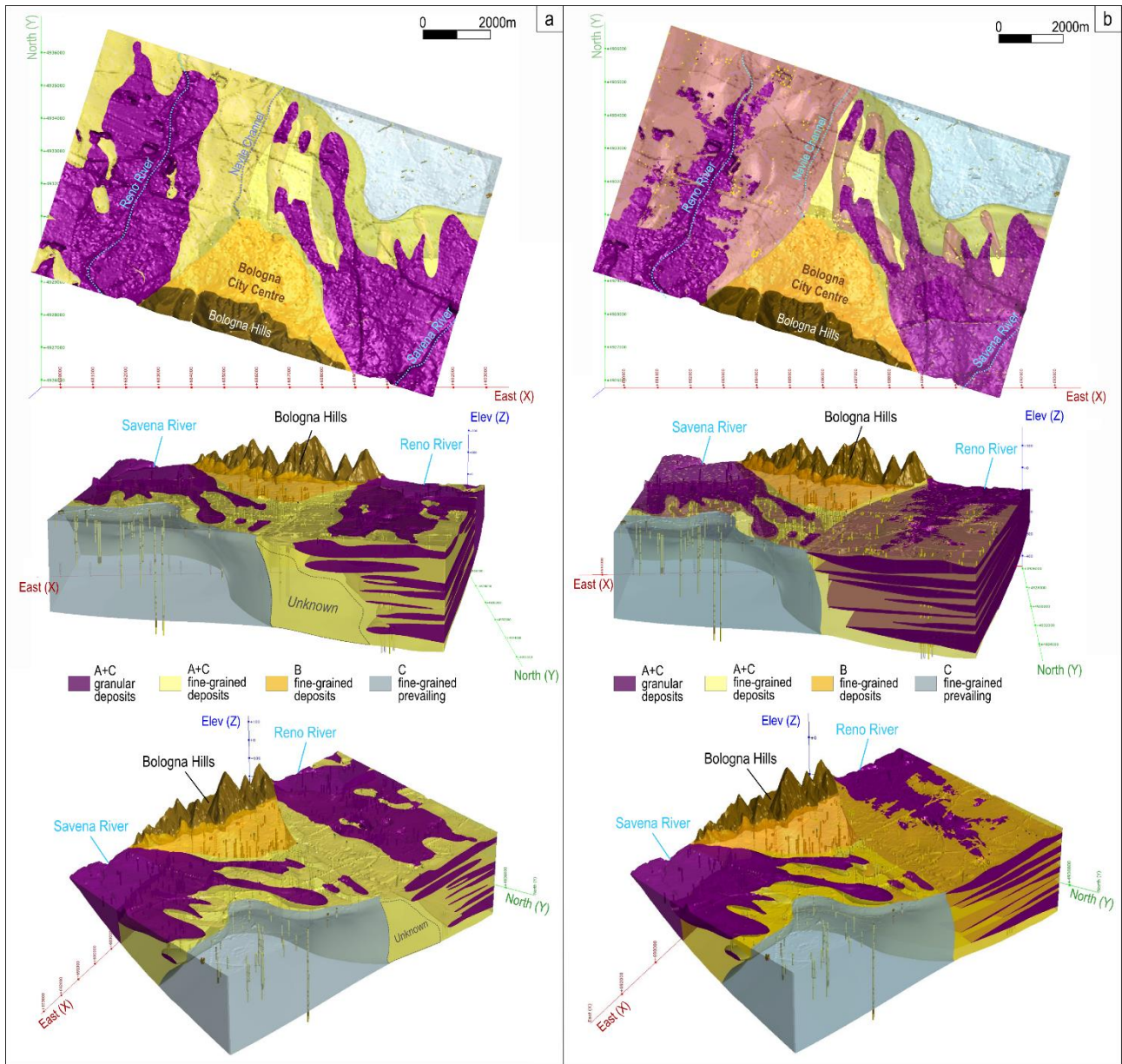


Figure 16- The 3D geological model of the Bologna urban area. In the Reno River domain (Domain A) the granular deposits were modelled within Leapfrog Works using both the “Intrusion” (a) and the “Deposit” tools (b).

#### 4.8 Geological interpretation

The different characteristics of Domains A, B, and C are likely related to the combined effect of fluvial and tectonic activity. The Reno River has a drainage basement about ten times larger than the Savena River (1060 km<sup>2</sup> vs 107 km<sup>2</sup> respectively) and it is mostly composed of clayey erodible rocks. A large catchment is expected to have a high capacity for sediment transport; therefore, the Reno River could have easily compensated for the uplift of the Apennine margin by cutting its deposits at the valley mouth. Moreover, the Reno River lies on the prolongation of a normal fault that flanks the lower reach of the valley (Picotti et



al., 2009, see Fig. 14). The possible presence of an extensional tectonic structure in the subsurface of the alluvial plain (Martelli et al., 2017) could explain the vertical amalgamation and confinement of the gravel bodies deposited by the Reno River, as well as the multi-stage sedimentation in a partially confined alluvial plain which finally resulted in the absence of a real fan. On the contrary, the limited transport capacity of the Savena River (possibly combined with the absence of active tectonic structures) could explain the convex fan morphology, the higher elevation of the apex, and the different internal architecture of the deposits. The prevalence of fine-grained soils beneath the historical centre of Bologna reflects instead the poor transport capacity of minor rivers draining the Apennine foothills. Here, the occurrence of vertically stacked paleosols indicates that Domain B was not involved in the fluvial dynamics of the Reno and Savena rivers, leaving this area essentially undisturbed.

## **5. Discussion**

### 5.1 General remarks on the lithofacies approach

Geological modelling of urban areas is typically based on stratigraphic correlation of borehole data. Although data density and quality are critical aspects for obtaining a reliable model, geological complexity is probably the most important issue. Cities built upon alluvial deposits, which are characterized by a high degree of heterogeneity and lateral facies changes, are much more complicated to model than cities settled, for example, upon coastal deposits where strata have greater areal continuity. In complex depositional environments, data is never enough, and the geological model may be uncertain even if the borehole density is very high.

The lithofacies approach, though time-consuming, was particularly effective in the subsurface of Bologna, where lithological correlation is difficult even over short distances, despite an average data density of 10 boreholes/km<sup>2</sup>. Here, stratigraphic analysis was combined with other types of data, including surface morphology, river network, and geophysical surveys. The lithofacies approach reduced the risk of correlating logs belonging to different depositional environments and led to the identification of three distinct depositional domains not recognized before (see Figs. 14, 16).

### 5.2 3D modelling or rendering?

In general, volume shaping within 3D modellers is based on the use of mathematical interpolators that spatially correlate stratigraphic data. We investigated the performance of automatic interpolation by comparing the two interpolators provided by Leapfrog Works named “Intrusion” and “Deposit” (see sect. 3.8). Despite the software offers a high degree of customization on these algorithms, neither was found fully suitable for our case. The “Intrusion” algorithm allows for a flexible shaping of the deposits that closely follows the stratigraphic data, but leaves uncovered large areas where data are absent (see Fig. 16 “Unknown” portion). The “Deposit” algorithm creates sheet-like volumes which extend far beyond the data, but over whose geometry the user has little control. In both cases, interpolation is by no means automatic and, at least in our complex geological setting, the 3D model cannot be totally entrusted to the software. That is why we first defined the geometry of sedimentary bodies using a dense grid of 2D stratigraphic sections, then we reproduced the inferred geometry by employing the most appropriate interpolator. As a matter of fact, in our complex case, the software was essentially used as a powerful 3D rendering tool rather than a real 3D modeller.

### 5.3 Geotechnical implications

3D geological models are essential tools, particularly in complex contexts with high latero-vertical lithostratigraphic variability such as the study area. These models not only condense and effectively display the general depositional architecture of the study area but also decisively support the analysis and interpretation of processes closely related to the geological setting. The 3D geological model, obtained exclusively through the stratigraphic analysis and the methodology described herein, has been, in fact, crucial in understanding the ongoing subsidence process evolution in the study area. Bologna experienced strong subsidence since the 1960s, due to groundwater pumping into the aquifers of the Reno and Savena rivers (Pieri & Russo, 1980; Brighenti et al., 1995; Bitelli et al., 2015). The subsidence reached in the early 1980s a peak of about 100 mm/year, then gradually decreased following the introduction of more restrictive regional pumping regulations (ARPAE, 2018). The geological model, however, which was developed independently from subsidence data, highlights a significant correspondence between the three identified depositional domains (i.e., A, B, and C) and the spatial distribution of the ground deformation field (Fig. 17). In the figure, the three identified domains are compared with the ground displacement maps obtained by topographic levelling (period 1983-1987, Barbarella et al., 1990) and by satellite interferometry from

ascending orbit RADARSAT data (period 2006-2011, ARPAE, 2012, Bitelli et al., 2014, 2015). Both the subsidence contour map (Fig. 17a) and the spatial distribution of punctual values obtained from radar interferometry (Fig. 17b) exhibit abrupt changes at the domains' boundary, especially at the limit between Domains A (Reno River) and B (Bologna city centre).

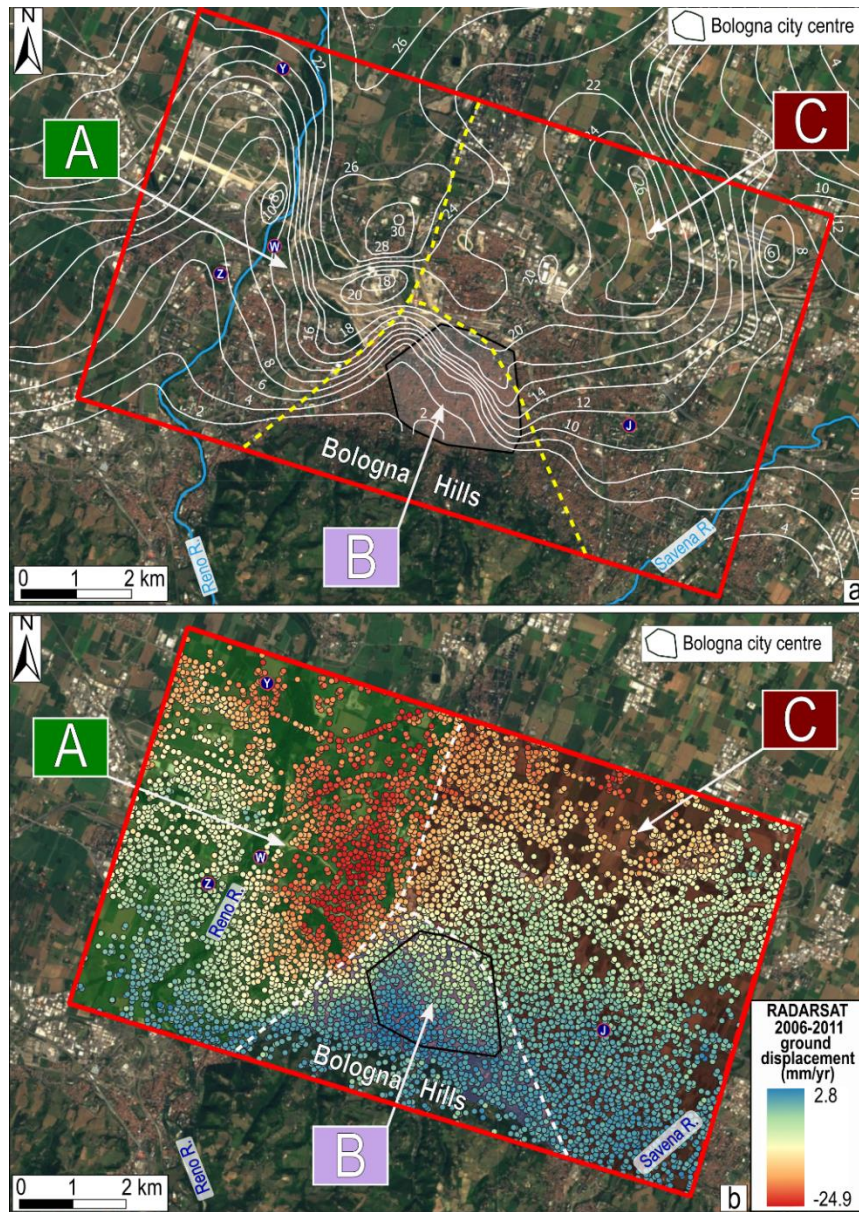


Figure 17- Comparison between the three domains identified in the geological model (A, B, and C) and ground displacement data: (a) the ground displacement map, measured in millimetres and reported as white contours, resulting from the 1983–1987 topographic levelling campaign (Barbarella et al., 1990); (b) the subsidence rate map, expressed in mm/year, from 2006–2011 Radarsat interferometric survey, displayed as coloured dots. The figure also includes the locations of the main wells' stations are also included: J- Fossolo; Y-San Vitale; W-Tiro a segno; Z-Borgo Panigale.

Moreover, the settlement field varies inside each domain according to their different stratigraphy. In Domain A (Reno River), the ground subsidence is relatively small in the proximal portion, where thick gravel bodies

are amalgamated and fine-grained layers are almost absent, and it increases downstream following the higher abundance of clayey deposits. The distal portion of this domain, characterized mostly by silty and clayey deposits, shows the highest subsidence rate. Similarly, within Domain C (Savena River) subsidence values are relatively small close to the fan apex and increase northward approaching the “fine-prevailing” area of the model. Interestingly, although composed mainly of fine-grained deposits, Domain B is characterised by small subsidence rates (see Fig. 16a). This apparent discrepancy is likely related to the peculiar features of Domain B, that according to the lithofacies analysis consists of stiff clay deposits (well-drained floodplain, WF) hosting frequent paleosols (Amorosi et al., 2017; Bruno et al., 2020). Ageing in secondary compression and periods of subaerial exposure may have resulted in the overconsolidation of the fine-grained deposits with a consequent increase in soil stiffness. Beside the lithostratigraphic analysis, a survey was conducted to gather information on available Cone Penetration Tests (CPTs) within the study area. A total of 593 CPTs were available, out of which 143 were digitised. The selection prioritised surveys deeper than 15 m and those located in areas with limited stratigraphic data coverage. Lithological data from these tests were systematically derived using either the Schmertmann (1970) or Robertson et al. (1986) classification methods, depending on the type of survey. Literature empirical relations were then employed to determine the main geotechnical parameters of the identified coarse and fine-grained layers. CPT surveys in Domains A and C, situated along the alluvial fans of the Reno and Savena rivers, are often shallow due to the presence of gravel. Consequently, the geotechnical characteristics of these sedimentary bodies, including both gravel deposits and the deeper clayey intervals between them, are generally unknown. On the contrary, the geotechnical characteristics of Domain B were investigated through several relatively deep penetration tests. Geotechnical data for Domain B were obtained from 31 digitised CPTs with depths ranging from 15 to 30 metres. The undrained shear strength ( $S_u$ ) profiles (Fig. 18) systematically exhibit relatively high values, ranging from 81 to 235 kPa on average, falling between the “Stiff” and “Very Stiff” fields of the soil consistency classification proposed by Terzaghi & Peck (1967).

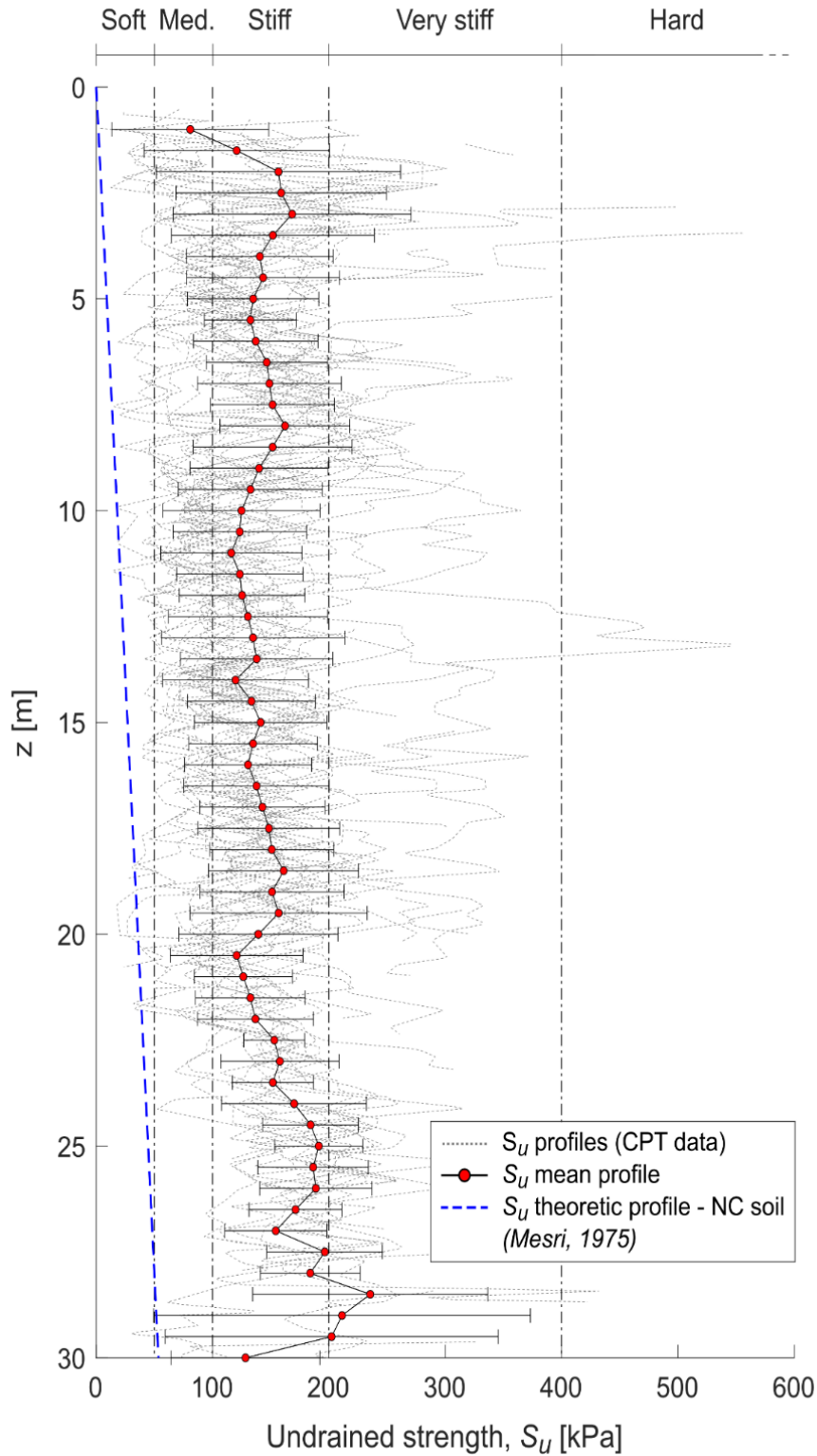


Figure 18- Comparison of undrained shear strength ( $S_u$ ) profiles in Domain B derived from CPT data. The  $S_u$  profiles were determined through the equation proposed by Robertson (2009):  $S_u = (q_t - \sigma_{v0})/N_{kt}$ , where  $q_t$  is the corrected cone resistance,  $\sigma_{v0}$  is the total overburden stress and  $N_{kt}$  is the cone factor, set to an average value of 14 after Robertson & Cabal (2015). The mean  $S_u$  profile (red dots) along with the corresponding standard deviation values is compared with the typical consistency values chart for fine-grained soils developed by Terzaghi & Peck (1967) and the theoretical trend for normally consolidated (NC) soils proposed by Mesri (1975):  $S_u = 0.22\sigma'_{v0}$ , where  $\sigma'_{v0}$  is the effective vertical stress.

Moreover, these high undrained strength values do not increase with depth and significantly diverge from the theoretical profile expected for normally consolidated (NC) soils, reported in Figure 18.

The 3D geological model effectively accounts for the existence of firm, overconsolidated clays beneath Bologna city. As mentioned earlier, Domain B seems to have remained unaffected by the fluvial dynamics of the Reno and Savena rivers, resulting in an undisturbed area where the material has become overconsolidated due to the combined effects of aging and drying. This is also evident from the abundance of paleosols found in this domain.

The simplification, for geotechnical purposes, of the obtained 3D geological model led to grouping different layers into two main types of deposits, that are coarse-grained and fine-grained deposits (see Fig. 16). However, the simplification process within a complex alluvial environment such as that of the study area, when guided by the lithofacies and their correlations, results in a more coherent and conscious approach. In fact, based on lithofacies correlations, it was possible to distinguish, as discussed above, three main domains with different depositional characteristics, underlying different ground surface behaviour, as also evidenced by subsidence data.

Further in-depth analysis of the geotechnical properties of the sedimentary bodies reconstructed in the 3D model and their relation to subsidence evolution, in view of a detailed numerical modelling analysis of the ground deformation process, is currently underway and will be deepened in future work.

## **6. Conclusions**

In this work, we present a 3D geological model of the Bologna urban area developed through a detailed surface (DTM, hydrography) and subsurface (geophysical surveys, boreholes) data analysis. A simplified geological model was built integrating surface morphology and subsurface stratigraphy, based on lithofacies correlation criterion, that guided the final 3D modelling.

Based on the findings of this study, the following conclusions can be drawn:

- 1) The lithofacies criterion proved to be an effective approach for reconstructing the urban subsurface in a complex alluvial setting; stratigraphic correlation guided by lithofacies provides a reliable representation of

sediment bodies and their geometry, overcoming the limitations of the lithologic approach commonly used in engineering geology.

2) The main difficulty of the lithofacies approach is the identification of the depositional facies based uniquely on log descriptions; re-interpreting borehole data, from lithology to lithofacies, requires time and specific sedimentological expertise.

3) The analysis allowed the definition of three different depositional domains with a common alluvial origin, but distinct morphological characteristics and depositional stacking patterns: the western part of the city (Domain A) lies over massive, thick gravel deposits that filled a subsiding alluvial valley; the central part (Domain B) is an interfluvial area dominated by stiff fine-grained soils that were essentially unaffected by the activity of the main rivers; the eastern part (Domain C) corresponds to a typical alluvial fan with gravel-dominated proximal deposits.

4) The three depositional domains guided the development of the 3D geological model and imposed to divide the bounding volume into three independently modelled sub-volumes; within each sub-volume, the geometry of sedimentary bodies was defined based on a dense grid of 2D stratigraphic cross-sections; no automatic algorithm proved to be really suitable to interpolate stratigraphic data in our complex case.

5) The 3D geological model showed a good agreement with the spatial distribution of the ground subsidence observed in Bologna since the 1960s, providing independent confirmation of the model itself.

## **Declaration of Competing Interest**

The authors declare no conflict of interest.

## **Acknowledgements**

This study was supported by the research grant URGENT - Urban Geology and Geohazards: Engineering geology for safer, resilieNt and smart ciTies funded by the Italian Government (Progetti di Ricerca di Rilevante Interesse Nazionale, PRIN2017, Prot. 2017HPJLPW). We thank Stefano Cremonini very much for his helpfulness and support.



## References

- Allen, J.R.L., 1963. The classification of cross-stratified units with notes on their origin. *Sedimentology*, 2, 93-114.
- Amorosi, A., Farina, M., Severi, P., Preti, D., Caporale, L., Di Dio, G., 1996. Genetically related alluvial deposits across active fault zones: an example of alluvial fan-terrace correlation from the upper Quaternary of the southern Po Basin, Italy. *Sediment. Geol.*, 10'2, 275–295.
- Amorosi, A., Caporale, L., Farina, M., Preti, D., Severi, P., 1997. Late Quaternary sedimentation at the southern margin of the Po Basin (Northern Italy). *Geologia Insubrica* 2, 149–159.
- Amorosi, A., Pavesi, M., Ricci Lucchi, M., Sarti, G., Piccin, A., 2008. Climatic signature of cyclic fluvial architecture from the Quaternary of the central Po Plain, Italy. *Sediment. Geol.* 209, 58–68.
- Amorosi, A., Bruno, L., Rossi, V., Severi, P., Hajdas, I., 2014. Paleosol architecture of a late Quaternary basin-margin sequence and its implications for high-resolution, nonmarine sequence stratigraphy. *Glob. Planet. Chang.* 112, 12–25.
- Amorosi, A., Bruno, L., Cleveland, D.M., Morelli, A., Hong, W., 2017. Paleosols and associated channel-belt sand bodies from a continuously subsiding late Quaternary system (Po Basin, Italy): new insights into continental sequence stratigraphy. *Geol. Soc. Am. Bull.*, 129, 449–463.
- Argnani, A., Barbacini, G., Bernini, M., et al. 2003. Gravity tectonics driven by Quaternary uplift in the Northern Apennines: insights from the La Spezia-Reggio Emilia geo-transect. In *Uplift and Erosion; Driving Processes and Resulting Landforms; Dynamic Relations Between Crustal and Surficial Processes*, Bartolini C, Piccini L, Catto NR (eds). *Quatern. Int.*, 13–26.
- ARPAE (Agenzia Prevenzione Ambientale Energia Emilia-Romagna), 2012. Rilievo della subsidenza nella pianura emiliano-romagnola - seconda fase, Bologna, 2018.
- ARPAE (Agenzia Prevenzione Ambientale Energia Emilia-Romagna), 2018. Rilievo della subsidenza nella pianura emiliano-romagnola - seconda fase, Bologna, 2018.

- Akkaya, İ., & Özvan, A., 2019. Site characterization in the Van settlement (Eastern Turkey) using surface waves and HVSR microtremor methods. *J. Appl. Geophys.*, 160, 157-170.
- Barbarella, M., Pieri, L. and Russo, P., 1990. Studio dell'abbassamento del suolo nel territorio bolognese mediante livellazioni ripetute: Analisi dei movimenti e considerazioni statistiche. *Inarcos*, 506, 1-19.
- Bitelli, G., Bonsignore, F., Del Conte, S., Novali, F., Pellegrino, I., Vittuari, L., 2014. Integrated use of advanced InSAR and GPS data for subsidence monitoring. In: Lollino G., Manconi A., Guzzetti F., Culshaw M., Bobrowsky P.T. and Luino F. (eds), *Engineering Geology for Society and Territory*, Springer, Berlin, Germany, Vol. 5, pp. 147-150, doi: 10.1007/978-3-319-09048-1\_29
- Bitelli, G., Bonsignore, F., Pellegrino, I., Vittuari, L., 2015. Evolution of the techniques for subsidence monitoring at regional scale: the case of Emilia-Romagna region (Italy), *Proc. IAHS*, 372, 315–321, <https://doi.org/10.5194/piahs-372-315-2015>
- Bridge, J.S., Jalfin, G.A., Georgieff, S.M., 2000. Geometry, Lithofacies, and Spatial Distribution of Cretaceous Fluvial Sandstone Bodies, San Jorge Basin, Argentina: Outcrop Analog for the Hydrocarbon-Bearing Chubut Group. *J. Sed. Res.*, 70 (2): 341–359. <https://doi.org/10.1306/2DC40915-0E47-11D7-8643000102C1865D>
- Brighenti, G., Borgia, G. C., Mesini, E., 1995. Chapter 5 Subsidence studies in Italy, Editor(s): Chilingarian G.V., Donaldson E.C., Yen T.F., *Developments in Petroleum Science*, Elsevier, Volume 41, 1995, Pages 215-283, ISSN 0376-7361, ISBN 9780444818201, [https://doi.org/10.1016/S0376-7361\(06\)80052-X](https://doi.org/10.1016/S0376-7361(06)80052-X).
- Bruno, L., Marchi, M., Bertolini, I., Gottardi, G., Amorosi, A., 2020. Climate control on stacked paleosols in the Pleistocene of the Po Basin (northern Italy). *J. Quaternary Sci*, 35, 559–571. <https://doi.org/10.1002/jqs.3199>
- Bruno, L., Amorosi, A., Severi, P., Bartolomei, P., 2015. High-frequency depositional cycles within the late Quaternary alluvial succession of Reno River (northern Italy). *Ital. J. Geosci.*, 134(2), 339–354. <https://doi.org/10.3301/IJG.2014.4>

- Bruno, L., Amorosi, A., Curina, R., Severi, P., Bitelli, R., 2013. Human–landscape interactions in the Bologna area (northern Italy) during the mid–late Holocene, with focus on the Roman period. *Holocene*, 23, 1560– 1571.
- Campo, B., Bruno, L., Amorosi, A., 2020. Basin-Scale Stratigraphic Correlation of Late Pleistocene–Holocene (MIS 5e–MIS 1) Strata across the Rapidly Subsiding Po Basin (Northern Italy). *Quat. Sci. Rev.*, 237.
- Carminati, E., & Di Donato, G., 1999. Separating natural and anthropogenic vertical movements in fast subsiding areas: the Po Plain (N. Italy) case. *Geophys. Res. Lett.*, 26: 2291–2294.
- Castellarin, A., Eva, C., Giglia, G., Vai, G.B., Rabbi, E., Pini, G.A., Crestana, G., 1985. Analisi strutturale del Fronte Appenninico Padano. *Giorn. Geol.* 47, 47–75.
- Castellaro, S., & Mulargia, F., 2009.  $V_{s30}$  estimates using constrained H/V measurements. *Bull. Seismol. Soc. Am.*, 99:761–773.
- Catuneanu, O., 2006. *Principles of Sequence Stratigraphy*, Elsevier, Amsterdam, 375 pp.
- Choobbasti, A.J., Rezaei, S., Farrokhzad, F., 2013. Evaluation of site response characteristics using microtremors. *Gradevinar*, 65: 731–741.
- Chiesa, A., 1742. *Carta topografica di tutta la pianura del Bolognese*, scala in miglia italiane.
- Cremonini, S., 1980. *Evoluzione morfologica della pianura bolognese tra Reno e Idice*. Tesi di laurea, Università di Bologna, inedita.
- Culshaw, M.G., & Price, S.J., 2012. The contribution of urban geology to the development, regeneration and conservation of cities. The 2010 Hans Cloos lecture. *Bull. Eng. Geol. Environ*, Volume 70, No 3, pp 333-376. doi 10.1007/s10064-011-0377-4.
- El May, M., Dlala, M., Chenini, I., 2010. Urban geological mapping: Geotechnical data analysis for rational development planning. *Eng. Geol.*, 116 (1-2), 129-138, <https://doi.org/10.1016/j.enggeo.2010.08.002>

- Elmi, C., Bergonzoni, A., Massa, T., Montaletti, V., 1984. Il territorio di pianura del Comune di Bologna: aspetti geologici e geotecnici. *Giornale di Geologia, Rivista di Geologia Sedimentaria e Geologia Marina*, 46, n. 2. ISSN 0017-0291.
- Fordyce, F.M., & Campbell, S.D.G, 2017. The Geosciences in Europe's Urban Sustainability: Lessons from Glasgow and Beyond (CUSP). *Earth and Environmental Science Transactions of the Royal Society of Edinburgh Special Issue*, 108 (2–3)
- Germani, D., & Angiolini, L., 2003. Guida Italiana alla classificazione e alla terminologia stratigrafica. *Quaderni, Difesa del Suolo, Serie III*, 9: pp. 155.
- He H.H., He J., Xiao J.Z., Zhou Y.X., Liu Y., Li C., 2020. 3D geological modeling and engineering properties of shallow superficial deposits: a case study in Beijing, China. *Tunn Undergr Sp Tech.*;100:103390, <https://doi.org/10.1016/j.tust.2020.103390>
- Geological Map of Italy 1:50.000 by the Geological Survey of Italy-ISPRA –Sheets: 220 Casalecchio di Reno-221 Bologna and Geological notes.
- Gunderson, K., Pazzaglia, F.J., Picotti, V., Anastasio, D.A., Kodama, K.P., Rittenour, T., Frankel, K.F., Ponza, A., Berti, C., Negri, A., Sabbatini, A., 2014. Unraveling tectonic and climatic controls on synorogenic growth strata (Northern Apennines, Italy). *Geol. Soc. Am. Bull.*, 126, 3/4: 532-552
- Hemmerle, H., Ferguson, G., Blum, P., Bayer, P., 2022. The evolution of the geothermal potential of a subsurface urban heat island. *Environ. Res. Lett.*, 17 (8).
- Hooimeijer, F.L., & Maring, L., 2018. The significance of the subsurface in urban renewal. *Journal of Urbanism: International Research on Placemaking and Urban Sustainability*, 11:3, 303-328, DOI: 10.1080/17549175.2017.1422532
- Huggenberger, P., & Epting, J., 2011. *Urban Geology. Process-Oriented Concepts for Adaptive and Integrated Resource Management*. Springer, Basel, <https://doi.org/10.1007/978-3-0348-0185-0>

- Kokkala, A., & Marinos, V., 2022. An engineering geological database for managing, planning and protecting intelligent cities: The case of Thessaloniki city in Northern Greece. *Eng. Geol.*, 301, <https://doi.org/10.1016/j.enggeo.2022.106617>
- Lapenna, V., Chambers, J., Shi, B., Lienhart, W., Zhu, H., 2020. Frontiers and applications of geological engineering and geophysical monitoring technologies in urban areas. *Eng. Geol.*, Special Issue, 268, <https://doi.org/10.1016/j.enggeo.2020.105508>
- Martelli, L., Bonini, M., Calabrese, L., Corti, G., Ercolessi, G., Molinari, F.C., Piccardi, L., Pondrelli, S., Sani, F. and Severi, P., 2017. Seismotectonic map of the Emilia-Romagna Region and surrounding areas, Scale 1:250,000, nd edn. D.R.E.AM, Firenze.
- Martorana, R., Capizzi, P., Avellone, G., D'Alessandro, A., Siragusa, R., Luzio, D., 2017. Assessment of a geological model by surface wave analyses, *J. Geophys. Eng.*, 14, 1, 159–172. <https://doi.org/10.1088/1742-2140/14/1/159>
- Mathers, S., Burke, H., Terrington, R., Thor, S., Dearden, R., Williamson, J., Ford, J., 2014. A geological model of London and the Thames Valley, southeast England. *Proceedings of the Geologists' Association*, 125(4): 373-382.
- Mesri, G., 1975. New design procedure for stability of soft clays. *Discussion, J. of the Geotech. Eng. Div., ASCE*, 101(4), 409-412.
- Miall, A.D., 1977. A review of the braided river depositional environment. *Earth Sci. Rev.*, 13 (1), 1-62.
- Miall, A.D., 1978. Lithofacies types and vertical profile models in braided river deposits: a summary *Canadian Society of Petroleum Geologists*, 52 (5), 597-604.
- Miall, A.D., 1985. Architectural-element analysis: A new method of facies analysis applied to fluvial deposits, *Earth-Science Reviews*, 22, Issue 4, 261-308. [https://doi.org/10.1016/0012-8252\(85\)90001-7](https://doi.org/10.1016/0012-8252(85)90001-7)
- Miall, A.D., 1996. *The geology of fluvial deposits: sedimentary facies, basin analysis and petroleum geology*. Berlin, Springer International, 582 p. <https://doi.org/10.1007/978-3-662-03237-4>
- Miall, A.D., 2016. *Stratigraphy: A Modern Synthesis*. Switzerland, Springer International, 454 p.

- Moisidi, M., Vallianatos, F., Kershaw, S., Collins, P., 2015. Seismic site characterization of the Kastelli (Kissamos) basin in northwest Crete (Greece): assessments using ambient noise recordings. *Bull. Earthq. Eng.*, 13, 725–753.
- Nakamura, Y., 1989. A method for dynamic characteristics estimation of subsurface using microtremor on the ground surface. *Q. Rep. Railw. Tech. Res. Inst.* 30:25–33.
- Ori, G.G., 1982. Braided to meandering channel patterns in humid-region alluvial fan deposits, River Reno, Po Plain (northern Italy). *Sediment. Geol.* 31, 231–248.
- Picotti, V., Ponza, A., Pazzaglia, F.J., 2009. Topographic expression of active faults in the foothills of the Northern Apennines. *Tectonophysics*, 474, 285–294.
- Pieri, M., & Groppi, G., 1981. Subsurface geological structure of the Po Plain, Italy. *P.F. Geodin. Publ.*, 414. C.N.R., Roma 1–23.
- Pieri, L., & Russo, P., 1980. Abbassamento del suolo della zona di Bologna: considerazioni sulle probabili cause e sulla metodologia per lo studio del fenomeno. *Collana di orientamenti geomorfologici ed agronomico-forestali*. Pitagora Editrice, Bologna, 1980.
- Posamentier, H.W., & Allen, G.P., 1999. Siliciclastic sequence stratigraphy— concepts and applications. *Concepts in sedimentology and paleontology*, SEPM Society for Sedimentary Geology, Tulsa, 7, 210 p. <https://doi.org/10.2110/csp.99.07>
- Price, S.J., Ford, J.R., Campbell, S.D.G., Jefferson, I., 2016. Urban Futures: the sustainable management of the ground beneath cities. In: *Developments in Engineering Geology* (Eggers et al., eds.), <https://doi.org/10.1144/EGSP27.2>.
- RER & ENI-AGIP, 1998. *Riserve idriche sotterranee della Regione Emilia-Romagna*. Bologna. A cura di G.M: DI Dio. S.EL.CA, Firenze, 120 pp.
- Ricci Lucchi, F., 1986. Oligocene to Recent foreland basins of Northern Apennines. In *Foreland Basins*, Allen P, Homewood P (eds). *International Association of Sedimentologists, Special Publications*, 105–139.

- Robertson, P. K., Campanella, R. G., Gillespie, D., Greig, J., 1986. Use of Piezometer Cone Data. Proceedings of the ASCE Specialty Conference on In Situ'86: Use of In Situ Tests in Geotechnical Engineering, Blacksburg, Virginia, 151–158.
- Robertson, P. K., 2009. Interpretation of cone penetration tests – a unified approach. *Can. Geotech. J.* 49 (11), 1337–1355.
- Robertson, P. K., & Cabal, K. L., 2015. Guide to Cone Penetration Testing for Geotechnical Engineering. Gregg Drilling & Testing, Inc. 6th Edition.
- Salvany, J. M., & Aguirre, J., 2020. The Neogene and Quaternary deposits of the Barcelona city through the high-speed train line. *Geologica Acta*, 18. [DOI: 10.1344/GeologicaActa2020.18.10]
- Schmertmann, J. H., 1970. Static cone to compute static settlement over sand. *JSMF Div. ASCE*, Vol.96 (3), 1011–1043.
- Seequent, 2019. User Manual for Leapfrog Works version 3.0.
- SESAME, 2004. Guidelines for the implementation of the H/V spectral ratio technique on ambient vibrations measurements, processing, and interpretation. In: SESAME European Research Project Wp12 – Deliverable d23.12, European Commission – Research General Directorate, Project No. EVG1-CT-2000-00026, [http://sesame.geopsy.org/Papers/HV\\_User\\_Guidelines.pdf](http://sesame.geopsy.org/Papers/HV_User_Guidelines.pdf) Accessed 21 Jun 2022
- Stafleu, J., Maljers, D., Gunnink, J.L., Busschers, F.S., 2011. 3D modelling of the shallow subsurface of Zeeland, the Netherlands, Netherlands. *J. Geosc.*, 16(1), 5647. <https://doi.org/10.5242/iamg.2011.0076>
- Terzaghi, K., & Peck, R.B., 1967. Soil mechanics in engineering practice, John Wiley, New York, NY, USA, p. 729.
- Thierry, P., Prunier-Leparmentier, A., Lembezat, C., Vanoudheusden, E., Vernoux, J., 2009. 3D geological modelling at urban scale and mapping of ground movement susceptibility from gypsum dissolution: The Paris example (France). *Eng. Geol.*, 105 (1–2), <https://doi.org/10.1016/j.enggeo.2008.12.010>

- Vail, P.R., Mitchum Jr., R.M., Thompson III, S. 1977. Seismic Stratigraphy and Global Changes of Sea Level, Part 4: Global Cycles of Relative Changes of Sea Level. In: Payton C.E. (Ed.). Seismic Stratigraphy — Applications to Hydrocarbon Exploration. AAPG Memoir, 26, 83-97.
- Van Wagoner, J.C., Mitchum, R.M., Campion, K.M., Rahmanian, V.D., 1990. Siliciclastic Sequence Stratigraphy in Well Logs, Cores, and Outcrops: Concepts for High-Resolution Correlation of Time and Facies. Mem. Am. Assoc. Pet. Geol. Memoir, 55 p. <https://doi.org/10.1306/Mth7510> Van Wagoner J.C.
- Velasco, V., Cabello, P., Vázquez-Suñé, E., López-Blanco, M., Ramos, E., Tubau, I., 2012. A sequence stratigraphic based geological model in the urbanized area of the Quaternary Besòs delta (NW Mediterranean coast, Spain). *Geologica Acta*, 10, 373-393.
- Volchko, Y., Norrman, J., Ericsson, L.O, Nilsson, K.L., Markstedt, A., Öberg, M., Mossmark, F., Bobylev, N., Tengborg, P., 2020. Subsurface planning: Towards a common understanding of the subsurface as a multifunctional resource. *Land Use Policy*, 90, 104316, <https://doi.org/10.1016/j.landusepol.2019.104316>
- Von der Tann, L., Sterling, R.L., Zhou, Y., Metje, N., 2019. Systems approaches to urban underground space planning and management – A review. *Underground Space* 5(2), DOI: 10.1016/j.undsp.2019.03.003
- Wornardt, W.W., 1993. Application Of Sequence Stratigraphy To Hydrocarbon Exploration. Paper presented at the Offshore Technology Conference, Houston, Texas, May 1993. doi: <https://doi.org/10.4043/7084-MS>



## **CRedit authorship contribution statement**

**Giacomelli S.:** Conceptualization, Methodology, Software, Writing – Original Draft, Visualization;  
**Zuccarini A.:** Software, Validation; **Amorosi A.:** Writing – Review & Editing; **Bruno L.:** Writing – Review & Editing; **Di Paola L.:** Investigation, Software; **Severi P.:** Data Curation, Writing – Review & Editing; **Martini A.:** Data Curation; **Berti M.:** Funding Acquisition, Supervision, Methodology, Writing – Review & Editing.

**Declaration of interests**

The authors declare that they have no known competing financial interests or personal relationships that could have appeared to influence the work reported in this paper.

The authors declare the following financial interests/personal relationships which may be considered as potential competing interests:

## **Highlights**

- The Bologna 3D model integrates geomorphological, stratigraphic, and geophysical data
- In complex alluvial systems lithofacies are crucial for stratigraphic correlations
- A preliminary 2D conceptual geological model was vital for a reliable 3D modelling
- 3 different geological domains were distinguished in an apparently homogeneous alluvial context
- The subsidence spatial distribution agrees with the 3 distinct geological domains